SURFACE FLASHOVER UNDER VARIOUS SURFACE CONDITIONS

by

BRADLEY ALLEN HANNUM, JR., B.S.E.E

THESIS

Submitted in partial fulfillment of the requirements
for the degree of Master of Science in Electrical Engineering at
The University of Texas at Arlington
May 2022

Arlington, Texas

Supervising Committee:

David A. Wetz, Supervising Professor
Rasool Kenarangui
Wei-Jen Lee

ACKNOWLEDGEMENTS

First and foremost, I'd like to express my deepest appreciation for my supervisor Dr. David Wetz for providing me the opportunity to pursue my M.S.E.E under his tutelage. His guidance and support, both professional and personal, helped me persevere the challenges faced. Thank you to Dr. Rasool Kenarangui and Dr. Wei-Jen Lee for their support as part of the thesis advisory committee. Thank you to everyone in the Pulsed Power and Energy Lab: Alexander Johnston, Cole Tschritter, Connor Hernandez, Hayden Atchison, Nicolaus Jennings, Tyler Scoggin, and Zachary Bailey. I greatly appreciate all your assistance, whether it be a helping hand or discussing designs and test plans. I will cherish my time in the lab always.

This work was supported by the US Naval Engineering Education Consortium (NEEC) under grant N00174-19-1-0030. The authors would like to thank NEEC and the Naval Surface Warfare Center – Dahlgren division for their support of this work. Any opinions, findings, and conclusions or recommendations expressed in this publication are those of the author and do not necessarily reflect the views of the US Office of Naval Research or the Naval Surface Warfare Center – Dahlgren division.

DEDICATION

Thank you to all of my friends and family who have helped me get to this point. I truly could not have done it without you.

To my sister, Anna – Your caring words and encouragement mean more than you could ever know. Thank you for always lifting me up and believing in me.

To my brother, Brian – You are without a doubt the hardest working person I know. Thank you for always giving me the motivation I need to keep going.

To my mother, Barbara – Words cannot express the support you've given me, through the good times and the bad. Thank you for always helping me see the light at the end of the tunnel and making sure I get there.

To my late father, Bradley Sr. – You always had the right words to say when I needed guidance. Thank you for knowing when I needed a push and when I needed a pull. The Jr. looks pretty sharp.

To my love, Hailey – After everything we've been through, we did it. Thank you for your unwavering support, for always being there for me, and helping me see things through.

TABLE OF CONTENTS

LIST OF TABLES

Table Page

LIST OF FIGURES

LIST OF ABBREVIATIONS

ASTM – American Society for Testing and Materials

CIGRE – International Council on Large Electric Systems

CTI – Comparative Tracking Index

EML – Electromagnetic Launch

ESDD – Equivalent Salt Deposit Density

IEC – International Electrotechnical Commission

MVDC – Medium Voltage Direct Current

NSDD – Non-soluble Deposit Density

PLC – Performance Level Category

SEE – Secondary Electron Emission

SEEA – Secondary Electron Emission Avalanche

UL – Underwriters Laboratory

UV - Ultraviolet

ABSTRACT

SURFACE FLASHOVER UNDER VARIOUS SURFACE CONDITIONS

Bradley Allen Hannum Jr., M.S.E.E

The University of Texas at Arlington, 2022

Supervising Professor: David A. Wetz

Electrical insulators are critical components used in every high voltage application whether it is operated continuously or in a pulsed mode. Bulk dielectric breakdown and surface flashover must be prevented in all use cases, especially those that occur in polluted environments. Though electrical standards have been written as a guide to prevent insulator surface flashover, such as Underwriters Laboratories (UL) 840, they are not directly applicable to applications where size and weight are critical. UL 840 experimental design is vague, does not consider all environments, and is written primarily with the electric power utilities in mind. The research presented here is aimed at studying surface flashover under polluted environments for comparison to the advice given by UL 840 and other similar standards. The aim is to provide the electrical community with insight into how to use these standards when size and weight are critical and over conservativeness does not support operational needs. Five different insulator materials have been subjected to different pollution levels, and their dielectric flashover strength has been studied across samples of three different widths. Experiments have been performed under continuously applied DC electric fields and for those in which breakdown occurred below 12 kV, similar experiments have

been performed under transiently applied electric fields for comparison. The experimental setup and the results obtained will be presented.

CHAPTER I

INTRODUCTION

Insulators play a crucial role in high-voltage electrical systems by preventing high voltage conductors from arcing. However, insulators can fail and allow this arcing to occur by bulk breakdown through the dielectric insulator or by tracking along the insulator surface. Either form of dielectric breakdown is undesirable, resulting in serious damage to the high voltage system, especially when the energy dissipated in the arc is high. There are several factors that impact an insulator's ability to maintain its dielectric strength including, but not limited to: the type of insulator, the geometry of the conductors in contact with the insulator, the ambient environment, and the condition, or level of pollution, of the insulator.

Dielectric surface flashover occurs when the electrical potential applied between two conductors separated by an insulator exceeds the dielectric strength and an electrical conduction path is created in the form of an arc along the surface of the insulator, bridging the two conductors. Dielectric breakdown is an unpredictable process and, while many theoretical aspects of it are well understood, there are many more that are not. In most cases, interpolation of relevant empirically collected data is used to predict breakdown thresholds during the engineering process. Many standards exist to characterize both the bulk breakdown strength as well as the surface tracking potential. Some of the standards relating to bulk breakdown include American Society for Testing and Materials (ASTM) D149, International Electrotechnical Commission (IEC) 60243, Underwriters Laboratories (UL) UL 746A, UL 840, ASTM D877, ASTM D120, and ASTM D178. To measure the bulk dielectric strength the insulator is usually sandwiched between two electrodes with a voltage applied. The method in which the voltage is applied as well as the material, pressure, and temperature of the ambient environment around the setup may vary and affect the outcome.

Bulk dielectric strength is measured as the potential when the material starts to conduct current. Bulk dielectric breakdown will not be studied further in this thesis.

The standards aimed at helping to prevent surface tracking are categorized under evaluation in dry, wet, and polluted conditions Those studying dry conditions include ASTM D495 [1], IEC 61621 [2], UL746A [3], and UL 840 [4]. Wet conditions standards include ASTM D2303, IEC 60587 [5], UL 746A, UL 840, ASTM D3638[6], and IEC 60112 [7]. Polluted and extreme standards include ASTM D2132 [8], IEC 60587, and UL 840. In the experiments performed to write these standards, electrodes are typically separated by a fixed distance and placed in contact with the insulator surface. Voltage is applied and the surface flashover potential is defined as that when arcing along the surface begins. In ASTM D495 and UL 746A high-voltage, low-current dry-arc experiments are performed to evaluate a material's resistance to surface tracking under a high-voltage, low-current arc at 12.5 kV and 10 - 40 mA. In ASTM D3638 and IEC 60112, the comparative tracking index (CTI) experiment is performed to evaluate a material's resistance to surface tracking within an intermittently wet environment up to 1000 VAC. In ASTM D2303, an inclined plane time-to-track experiment evaluates a material's resistance to surface tracking under constantly wet contaminated conditions up to 6000 VAC. In ASTM D2132, the dust-and-fog tracking and erosion resistance of a material in a continually wet and dusty environment is measured. This is the harshest of the most common track resistance tests, and it also evaluates surface tracking and erosion through the material. A brief overview of some of the standards investigated is given below in Table I.

There are many similarities and many differences in the way in which these standards are drafted. Each has its own level of detail describing the experimental setup and methods used to collect the data and draft the guidance. This often makes them difficult to understand and even

more difficult to apply. So much of the detail of the standards listed above is still unclear and this thesis will not attempt to fill in those voids. Instead, it will thoroughly present a series of surface flashover experiments and the data collected from them. The results will be compared with those in the standards as they can, and the reader is able to infer from those results the relevance to their application.

Table I – Some standards comparisons

Standard	Purpose	Positives	Negatives	Notes
UL 840	Provides creepage and clearance requirements	• Extensive guidelines • Provides creepage and clearance examples	• Vague pollution degrees, no examples • Uses CTI value for material grouping • No test procedure background for data	• Designed for long-term stress • Outsources CTI testing to UL 746A • States data is empirical
UL 746A	Describes various mechanical, electrical, and ignition tests for polymeric materials	• Extensive testing for mechanical properties (impact, flex, shear, deflection, pressure) • CTI testing overview	• Convoluted test procedures • Minimal background information for procedures covered	• Outsources CTI testing to ASTM D495 • Lists CTI categories • References CTI voltage limitations (600V)
UL 746C	Describes various test procedures for polymeric materials used in electrical equipment	• Specific to usage in electrical equipment (enclosures, insulating, flammability) • Simplified flow chart application	• Covers very specific applications	• References CTI voltage limitations (600V) • Outsources inclined plane testing to ASTM D2303
ASTM D495	Outlines test procedure for determining CTI	• Useful for general material comparisons	• Severely limited applications and restrictions • Confusing test apparatus and procedure	• States that test data should *not* be used in material specifications or arc resistance rankings
ASTM D2132	Testing to define the tracking susceptibility of insulating materials	• Simplified specimen rankings of tracking resistant, tracking affected, tracking susceptible	• Specific to long-term material tracking	• Useful for testing multiple samples multiple times for direct comparison between materials
ASTM D2303	Evaluation of relative tracking and erosion resistance of insulating solids	• Useful for categorizing insulating materials for indoor or outdoor use	• Confusing test apparatus and procedure • No background reference data • Specific to long-term tracking	• States that comparative behaviors inferences should *not* be derived from the tracking test results
IEC 60112	Test procedures for determining comparative tracking indices of solid insulating materials	• Short term tracking testing	• Difficult test procedure • Limited to 600V testing	• Slightly modified copy of ASTM D495

CHAPTER II

BACKGROUND

High voltage engineers often must evaluate the dielectric strength of several materials before the right one is chosen for their application. Insulators exist in the form of solids, liquids, and gases. In liquids and gases, it's only possible for dielectric breakdown to occur through the bulk material or along interfaces where different forms of insulators come together. In the case of solid dielectrics, bulk dielectric breakdown through the material can occur but a phenomenon known as surface flashover is also possible where an electrical arc occurs along the surface of the insulator. Figure 1 displays various methods of electrical breakdown as a function of time; Table II lists various breakdown mechanisms of solid and gaseous dielectrics. The bulk dielectric breakdown strength of an insulator and/or its comparative tracking index (CTI) value is often given in the manufacturer's datasheet, though the values given are usually only validated under limited applied DC or AC conditions defined by a standard or their own unique testing procedure. The lack of consistent material property data and understanding of how the data was collected makes it difficult for the user to apply the standard without significant doubt. Aside from the use of electrical standards documented to help design towards the prevention of surface flashover, there is no other published manufacturer data that can be used to prevent its occurrence. Engineers must often perform their own experiments to validate the materials they are considering and the design choices they are making while attempting to conform to the industry standards deemed applicable.

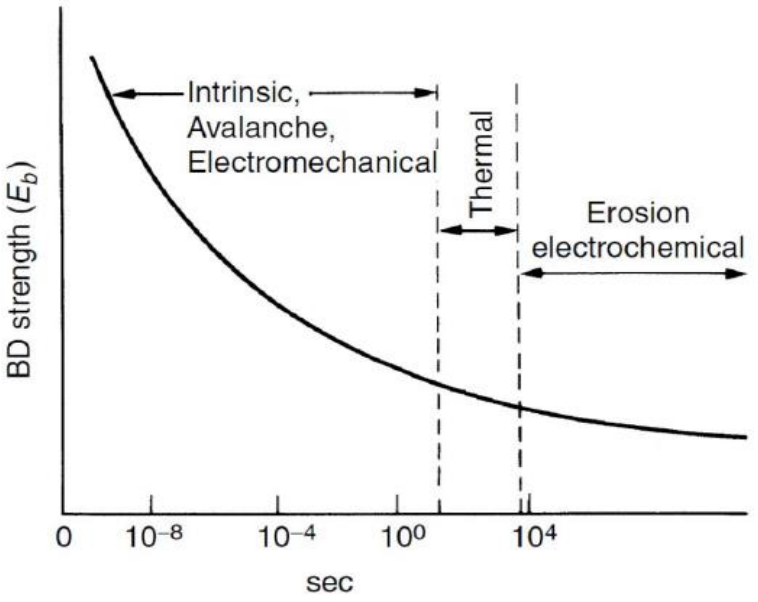

Figure 1 - Methods of electrical breakdown as a function of time [9, 10]

Table II – Different breakdown mechanisms [9, 10]

Breakdown Process	Solid Dielectrics	Gaseous Dielectrics
Electronic Breakdown	• Breakdown occurs in 10^{-8} s • Electrons in valence band move to conduction band	• Breakdown occurs due to electron avalanche from cumulative ionization
Streamer Breakdown	• Observed when electric field is highly non-uniform	• Occurs when ion concentration is high (10-8 cm^{-1}) • Breakdown is faster than avalanche mechanism
Thermal Breakdown	• Breakdown occurs in 0 to 10^{-3} seconds • Heat generated by electric field causes electron avalanche	
Breakdown by Tracking	• Breakdown can occur after several days or weeks • Solid insulator is exposed to electrical stresses for a long time	• The gas exposed to the insulator surface and gaseous byproducts of degrading insulators (e.g., pyrolysis) play a role in tracking degradation
Breakdown by Treeing	• Insulator is damaged through partial discharges and damage slowly progresses through the solid forming tree-like structures • Originates at impurities and gas voids in the insulator	
Breakdown by Surface Flashover	• Breakdown can take less than a second to days • Several reasons such as contamination of insulator, overheating, and change in surface charge could lead to breakdown	• Breakdown voltage also depends on type and pressure of gas exposed to insulator surface

2.1 Surface Flashover

When sizing insulators for a high voltage application the phenomena of creepage and clearance must be considered, defined in Figure 2, and prevented. Clearance must ensure the separation of the conductors is such that a bulk dielectric breakdown cannot occur directly through the insulator. Surface flashover occurs when the electrical potential applied between two conductors, separated by an insulator, exceeds the dielectric strength and an electrical conduction path is created in the form of an arc along the surface of the insulator, bridging the two conductors.

Figure 2 – Difference between creepage and clearance [11]

Most of the literature in this field of study has been performed to study the surface flashover of the ceramic insulators used to separate high voltage AC power lines [12-14]. A few photographs showing dielectric flashover of these components are shown in left and right photos in Figure 3 below. Due to the sheer number of power lines across the world and the people their operation affects, it makes sense that significant effort has gone into preventing flashover of these components. Figure 3 shows how even increasing the path length with a ribbed feature does not always prevent surface flashover from occurring (left), and significant damage when it does (right). There have also been quite a few studies performed evaluating dielectric flashover of electrical insulators in pulsed power applications, though most have been performed in a vacuum environment, discussed later. There is little literature describing the impact of surface pollutants

on the voltage at which surface flashover begins.

Figure 3 – Photograph of surface flashover occurring [12] (left) and its results [13] (right) on high voltage power line ceramic insulators

There are many theories behind the cause of surface flashover, most of which suggest that secondary electron emission is responsible. Dielectric breakdown can be divided into three stages: (1) initiation, (2) development, and (3) final stage [14]. It is generally agreed that the electron emission from the triple point is the initiating event in surface flashover. It is also generally agreed that the final stage discharge develops in a layer of desorbed gas from the surface [15]. The bulk of the literature studying surface flashover phenomena in pulsed power applications has been studied in vacuum environments [16-20] with few being performed in atmospheric conditions [14, 21-23] and a few in unique environments such as submersed in oil, or in cryogenic conditions [23-27]. None of those found were performed in a sea environment, and given the findings of [22, 23], it is clear that humidity plays a large role in surface flashover, suggesting that a salt fog environment will play a significant role in altering the surface flashover potential. The processes involved in the development stage are the subject of a range of differing theories. In his thesis, John Krile documents a thorough literature review of studies previously performed researching surface flashover phenomena which will be considered heavily in the proposed series of experiments presented herein [14].

Although the flashover process is thought to have the same three stages in an air environment, the manifestation of the stages very likely differs from those in vacuum. The initiation stages between the two processes are comparable, as the initial electrons are emitted from the triple point due to field enhancements. The combined processes of electron ionization, photo-ionization, UV induced SEE, SEEA across the surface, and Townsend amplification all contribute to streamer production as part of the development stage [14]. However, it's still unclear what roles these processes play in surface flashover or how much each one contributes. The streamer ionization channel bridges the gap in the final stage, initiating breakdown. Surface breakdown arcs are known to follow electric field lines in a vacuum environment; when a dielectric surface is present, however, the arc will follow that surface instead [14]. It's still unclear which of the multiple processes of dielectric breakdown or surface flashover contribute to this inclination to follow the surface in an air environment. The same is true in air, where the presence of the surface reduces the breakdown voltage greatly. [14]

In his thesis, Krile identified the impact that UV generated during breakdown in an air environment has on the emission of secondary electrons and the affect the net positive surface charge has on the arc following the surface. In a nitrogen environment Krile showed that an absence of UV caused the arcs to follow the electric field lines rather than the surface. He also showed that humidity has a significant effect on the surface flashover potential, showing that at 90% relative humidity the breakdown voltage is nearly half of what it is at 10% humidity in both air and nitrogen environments. It is important to note that Krile’s research was focused on DC breakdown and did not utilize contaminated surfaces.

Several models have been developed to attempt to predict a mathematical approach to surface flashover. The Obenaus model, proposed in 1958, was developed to simplify and quantify

the flashover process, and is often used as a baseline for other models used for alternative conditions [28 - 30]. As seen in Figure 4, The surface flashover is modelled as a discharge in series with the surface resistance of the insulator, representing the bridging of the dry band with the unbridged polluted portion of the insulator.

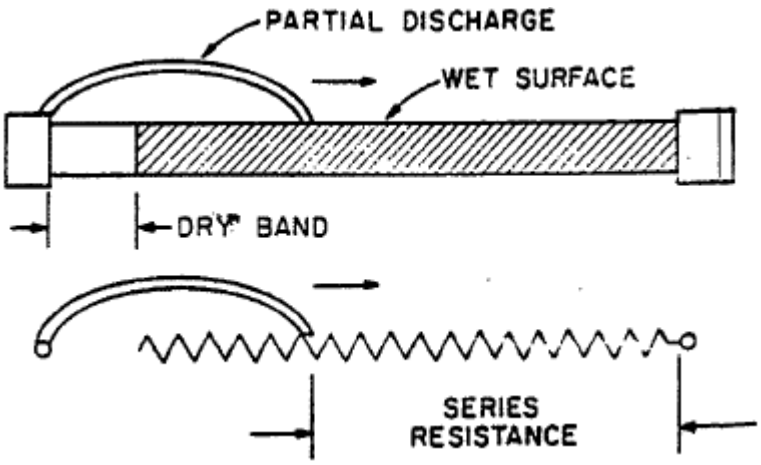

Figure 4 – Obenaus flashover model [30]

The breakdown voltage, $U_{BD,}$ for Obenaus's flashover model is given as

$$U_{BD} = AXI^{-n} + R_P I \tag{1}$$

where *A* and *n* are defined as characteristic constants, *X* is the arc length, *I* is the current, and R_P is the resistance of the pollution layer. When the voltage applied to the system exceeds the breakdown voltage the flashover process begins.

When polluted, the process for flashover is described in six phases, though some of the phases can occur concurrently [31]. The properties of the insulator affect the conditions, such as the CTI of the insulator and whether the surface is hydrophilic or hydrophobic. Hydrophilic surfaces will form an even layer of film across the surface under wetting conditions, whereas water

on a hydrophobic surface forms distinct water droplets. The process below is described for hydrophilic surfaces:

Phase 1: The surface of the insulator becomes polluted.

Phase 2: The surface of the polluted insulator becomes wetted. Pollutants that are non-conductive when dry become conductive when wet.

Phase 3: The conductive surface pollution layer on an energize insulator allows current leakage to flow. The current leakage heats and dries the surface of the insulator where the current density is highest; this results in the formation of dry bands.

Phase 4: The surface pollution layer does not dry uniformly. The conducting path is broken by dry bands which interrupts the flow of the leakage current.

Phase 5: The charge voltage appears across the dry bands causing air breakdown. The dry bands are bridged by arcs, with each dry band bridge appearing electrically in series with the resistance of the undried conductive pollution layer.

Phase 6: The arcs across the dry bands continue across the insulator until the entire surface is bridged, seen in Figure 6, establishing the line to ground, and inducing flashover.

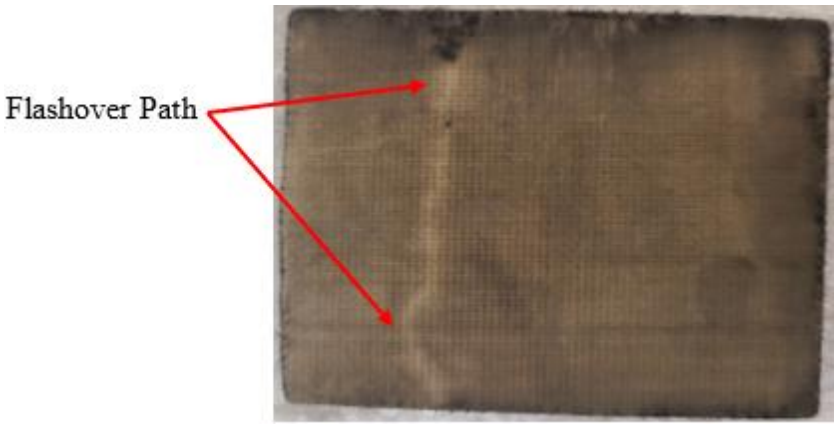

Figure 5 – Polluted sample showing the path of surface flashover

2.2 Surface Flashover Standards

In standards, the surface flashover potential is often presented for AC and DC voltage conditions. That is because when fields are applied in an alternating manner, the dielectric strength may vary considerably compared with DC potentials. When the slew rate increases further, applying voltage in a near transient manner, the strength may vary even further. Prevention of surface flashover may be difficult without drastically oversizing the design, as there are few manufacturer ratings that can be used in the design phase to prevent flashover in all circumstances. When size is not critical, it is easier to prevent bulk and surface breakdown of an insulator by simply sizing it such that the dielectric strength well exceeds the demands of the system; this freedom is not possible in compact power system designs size. Environmental factors, which can be as simple as dust on the surface, humidity, or salt in the air can severely degrade the dielectric strength, causing surface flashover to occur at lower-than-expected voltages.

Surface tracking of an insulator is evaluated under two separate conditions: dry tracking and wet tracking. The dry tracking evaluation method is used to determine the high-voltage, low current dry arc resistance performance level category (PLC) of solid electrical insulation [1, 3]. The high-voltage, low current arc-resistance test is intended to approximate service conditions in high-voltage AC circuits with current limited to less than 0.1 A. This testing excludes the addition of pollutants or contaminants to baseline the material tracking properties. ASTM D495 lists four general types of failure as occurring as part of the test procedure. The first failure listed occurs in inorganic dielectrics, where they become incandescent and become capable of conducting the current. Upon cooling, the dielectric returns to its earlier insulating conditions. The second failure applies to organic compounds, where they burst into flame without a visible formation of a conducting path on the substance. The third failure encountered is that of surface tracking, where

a thin line is formed on the surface of the insulator between the two electrodes. The fourth failure expected is that of surface carbonization which occurs until sufficient carbon is present to carry the current. Failures of any of the four listed types typically occur within the first few seconds after a change in severity stage, which will be described later.

The ASTM D495 Dry Arc test procedure allows for the use of a pair of either stainless steel or tungsten rod electrodes, each resting independently on the surface of the insulator at a 45º angle and spaced 0.250 ± 0.003 in. (6.35 ± 0.08 mm) apart from each other. The surface of each sample is conditioned using a cloth containing water or other suitable solvent, and then wiped with a clean dry cloth immediately before testing. The conditioned samples are placed into the electrode holder assembly where an adjustable transformer is set to provide 12,500 V. A test sequence consisting of 60-second steps is followed in which the specimen is subjected to increasing severity of arcing; this is accomplished by first increasing the duration of the arc, and in the later steps increasing current. The dry arc resistance of the material is determined by the total elapsed time of arcing exposure until tracking occurs. The steps listed refer to the inclusion of current control resistors which are switched in and out of the test apparatus as per the procedure. They can be seen below in Figure 6, listed as R10, R20, R30, and R40.

Table III – ASTM D495 test sequence [1]

Step	**Current (mA)**	**Time cycle (s)**	**Total time (s)**
1/8 – 10	10	1/4 on, 1-3/4 off (Interrupted arc)	60
1/4 – 10	10	1/4 on, 3/4 off (Interrupted arc)	120
1/2 - 10	10	1/4 on, 1/4 off (Interrupted arc)	180
10	10	Continuous	240
20	20	Continuous	300
30	30	Continuous	360
40	40	Continuous	420

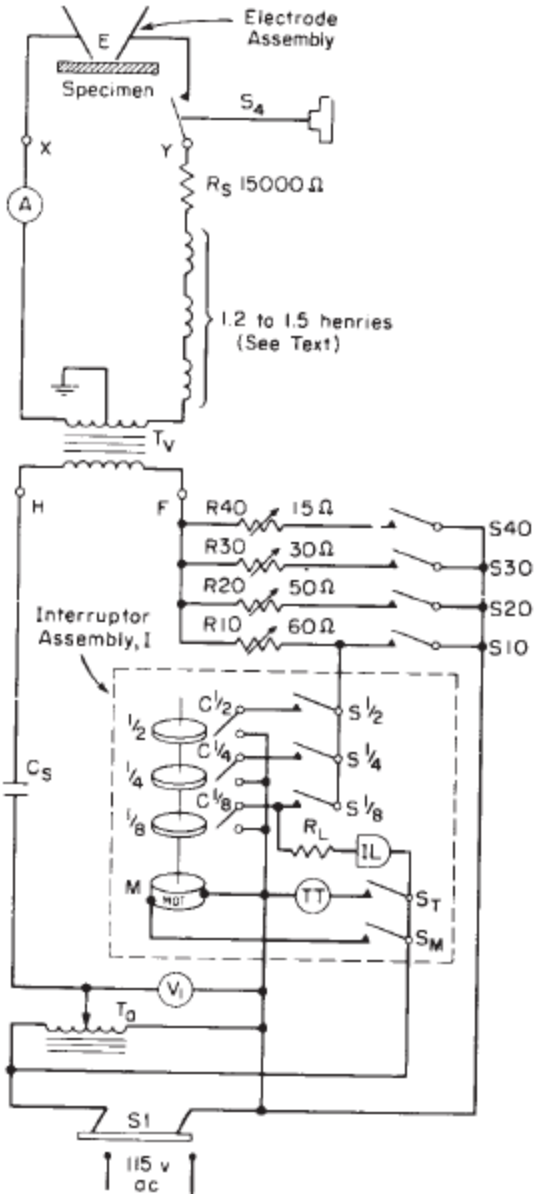

Figure 6 – ASTM D495 arc-resistance test circuit [1]

The alternative to the dry tracking test is the wet tracking test. In a wet CTI test, a DC voltage is applied to two platinum electrodes that are touching the insulator surface and separated by roughly 4 mm. In IEC 60112, drops of 0.1% ammonium chloride are dropped onto the surface of the insulator between the two electrodes from a height of 35 mm, and the CTI is defined as the voltage which causes tracking after 50 drops have fallen on the material. A drawing representative

of the setup along with a photograph of a commercial test stand is shown in Figure 7. It is the maximum voltage at which five specimens withstand the test period, typically 25 s, for 50 drops without failure and whether, at a voltage of 25 V lower than the maximum 50 drop figure, the specimen withstands 100 drops. If this is not the case, the maximum 100 drop withstand voltage must be determined. The voltage range between which tracking occurs defines its PLC and its material group as shown in Table III. The CTI value is often published in material datasheets but consultation of several different data sheets for the same material often finds widely different CTI values making it difficult to use the data with any confidence.

Table IV – Relationship between UL 840 Material Group, PLC, and CTI values [1, 3, 4, 7]

UL 840 Material Group	CTI Value	PLC Value
I	600 V ≤ CTI	0
II	400 ≤ CTI < 600	1
IIIa	250 ≤ CTI < 400	2
IIIa	175 ≤ CTI < 250	3
IIIb	100 ≤ CTI < 175	4
Not Defined	CTI < 100	5

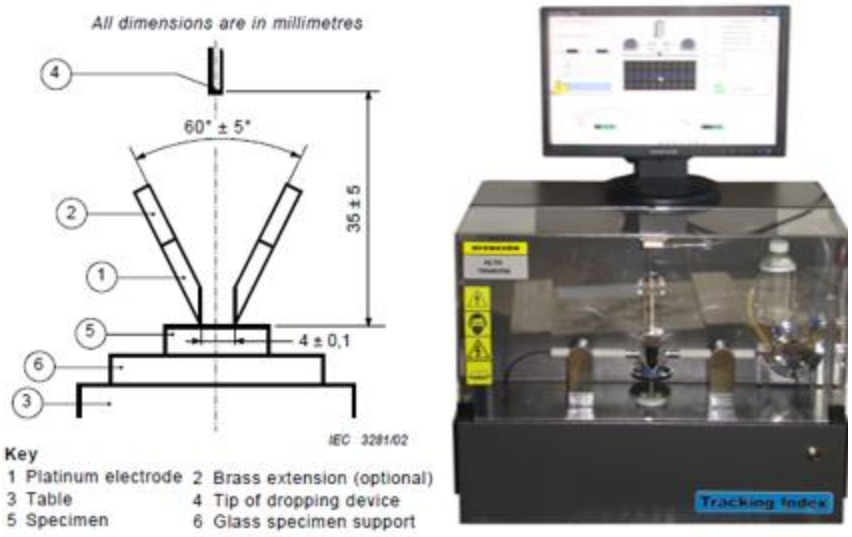

Figure 7 – Test apparatus used to measure an insulator's wet CTI. Dimensioned drawing from IEC 60112 (left) [7] and photograph of a commercially sold test system by SECOM (right) [32]

In the work performed here, a unique series of experiments has been performed to study the surface flashover potential of five different insulators under various levels of pollution. The materials studied include G9, G10/FR4, G11/FR5, polycarbonate, and Delrin®, and they were chosen due to their frequent usage in high voltage experiments. Below is a description of each material, and a summary of their electrical properties is provided in Table IV.

G9 (Glass-Melamine Laminate): A woven glass fabric that is very hard, flame resistant, and of machining grade with excellent electrical properties in high humidity conditions. It has high physical strength and excellent arc resistance [33].

G10/FR4: A thermosetting industrial laminate consisting of a continuous filament glass cloth material with an epoxy resin binder. It has characteristics of high strength, excellent electrical properties, and chemical resistance, not only at room temperature but also under humid or moist conditions. G10/FR4 glass epoxy laminate meets the specifications of Mil-I-24768/27, LP 509 & MIL P 18177 Type GEE [34].

G11/FR5: A glass-cloth reinforced epoxy that is like G10/FR4 but has a higher operating temperature and superior mechanical properties at elevated temperatures [35].

Polycarbonate: A plastic offering superior durability, design flexibility, and structural integrity that easily surpasses laminated glass and acrylic alternatives. Polycarbonate sheet (Standard General-Purpose Glazing Grade) will transmit 86% of light, is UV stabilized, and has a heat deflection temperature of 270°F at 264 PSI [36].

Delrin®: A plastic that has many of the same characteristics of industrial metals such as brass, aluminum, zinc, and stainless steel. It is a homopolymer acetal (POM) with properties that include stiffness, dimensional stability, impact resistance, and structural strength [37].

Table V – Electrical properties of the five different insulator types studied here

	G9	**G10/FR4**	**G11/FR5**	**Polycarbonate**	**Delrin®**
Permittivity (F/m)	6.3 [38]	5.0 [40]	4.5 [43]	2.7 – 3.4 [45]	3.9 [48]
Bulk Dielectric Strength (kV/mm)	11.8 [38]	31.5 [40]	35.4 [43]	11.8 – 38.0 [45]	45.0 [48]
Dry Arc Resistance (sec)	180 [38]	100 [40]	120 [43]	30 - 120 [45] 120 [46]	220 [49]
CTI (V)	600 [39]	300 [41] 175 [42]	150 [44]	85 - 600 [45] 100 – 400 [46] 121 – 256 [47]	600 [48]
Material Group	I	IIIa	IIIb	I, II, IIIa, or IIIb	I

Table VI – Minimum acceptable creepage distances [4]

Operating voltage, volts ac rms or dc[z]	Creepage distances for equipment subject to long-term stress, mm										
	Pollution degree 1	Pollution degree 2			Pollution degree 3				Pollution degree 4		
	All material groups	Material group[x]			Material group[x]				Material group[x]		
		I	II	IIIa,b	I	II	IIIa	IIIb	I	II	IIIa
10	0.08	0.4	0.4	0.4	1.0	1.0	1.0	1.0	1.6	1.6	1.6
12.5	0.09	0.42	0.42	0.42	1.05	1.05	1.05	1.05	1.6	1.6	1.6
16	0.1	0.45	0.45	0.45	1.1	1.1	1.1	1.1	1.6	1.6	1.6
20	0.11	0.48	0.48	0.48	1.2	1.2	1.2	1.2	1.6	1.6	1.6
25	0.125	0.5	0.5	0.5	1.25	1.25	1.25	1.25	1.7	1.7	1.7
32	0.14	0.53	0.53	0.53	1.3	1.3	1.3	1.3	1.8	1.8	1.8
40	0.16	0.56	0.8	1.1	1.4	1.6	1.8	1.8	1.9	2.4	3.0
50	0.18	0.6	0.85	1.2	1.5	1.7	1.9	1.9	2.0	2.5	3.2
63	0.2	0.63	0.9	1.25	1.6	1.8	2.0	2.0	2.1	2.6	3.4
80	0.22	0.67	0.95	1.3	1.7	1.9	2.1	2.1	2.2	2.8	3.6
100	0.25	0.71	1.0	1.4	1.8	2.0	2.2	2.2	2.4	3.0	3.8
125	0.28	0.75	1.05	1.5	1.9	2.1	2.4	2.4	2.5	3.2	4.0
160	0.32	0.8	1.1	1.6	2.0	2.2	2.5	2.5	3.2	4.0	5.0
200	0.42	1.0	1.4	2.0	2.5	2.8	3.2	3.2	4.0	5.0	6.3
250	0.56	1.25	1.8	2.5	3.2	3.6	4.0	4.0	5.0	6.3	8.0
320	0.75	1.6	2.2	3.2	4.0	4.5	5.0	5.0	6.3	8.0	10.0
400	1.0	2.0	2.8	4.0	5.0	5.6	6.3	6.3	8.0	10.0	12.5
500	1.3	2.5	3.6	5.0	6.3	7.1	8.0	8.0	10.0	12.5	16.0
630	1.8	3.2	4.5	6.3	8.0	9.0	10.0	10.0	12.5	16.0	20.0
800	2.4	4.0	5.6	8.0	10.0	11.0	12.5	y	16.0	20.0	25.0
1000	3.2	5.0	7.1	10.0	12.5	14.0	16.0	y	20.0	25.0	32.0
1250	4.2	6.3	9.0	12.5	16.0	18.0	20.0	y	25.0	32.0	40.0
1600	5.6	8.0	11.0	16.0	20.0	22.0	25.0	y	32.0	40.0	50.0
2000	7.5	10.0	14.0	20.0	25.0	28.0	32.0	y	40.0	50.0	63.0
2500	10.0	12.5	18.0	25.0	32.0	36.0	40.0	y	50.0	63.0	80.0
3200	12.5	16.0	22.0	32.0	40.0	45.0	30.0	y	63.0	80.0	100.0
4000	16.0	20.0	28.0	40.0	50.0	56.0	63.0	y	80.0	100.0	125.0
5000	20.0	25.0	36.0	50.0	63.0	71.0	80.0	y	100.0	125.0	160.0
6300	25.0	32.0	45.0	63.0	80.0	90.0	100.0	y	125.0	160.0	200.0
8000	32.0	40.0	56.0	80.0	100.0	110.0	125.0	y	160.0	200.0	250.0
10000	40.0	50.0	71.0	100.0	125.0	140.0	160.0	y	200.0	250.0	320.0

[w] Linear interpolation of the values is permitted.
[x] See 6.2.
[y] Material group IIIb shall not be used for application in pollution degree 3 above 630 volts.
[z] It is appreciated that tracking or erosion will not occur on insulation subjected to a working voltage of 32 volts and below. However, the possibility of electrolytic corrosion has to be considered, and for this reason, minimum creepages have been specified.

Table VI, taken from the UL840 standard, lists the minimum acceptable creepage distance for each material group and pollution degree, with operating voltages from 10 - 10,000 V. The table does allow for linear interpolation of the values, which will be used later in the discussion of

the results.

A key takeaway from the insulator electrical properties with comparison to the standards investigated is the uncertainty and oftentimes varying results for CTI, arc resistance, and material groupings. For example, datasheets from different manufacturers of polycarbonate list various CTI values that place the material in such a large grouping that it can be classified as any of the UL 840 Material Groups, assigning it in groups I, II, IIIa, or IIIb. At 10 kV the difference in grouping between Group I and Group IIIa (IIIb is not to be used above 630 V) is between 1.3 – 2.0 times the minimum allowable clearance distance depending on the level of pollution; at pollution degree 4 the difference in clearance is 120.0 mm, a significant distance when working in the confined spaces of shipboard environments. Obtaining a CTI value requires that a wet CTI test, as defined in IEC 60112, be performed on the actual material that is intended for use; this can become costly and time consuming.

The applicability of some of the standards is brought into question within the standards themselves. From ASTM D495:

> The usefulness of this test method is very severely limited by many restrictions and qualifications. Generally, this test method should *not* be used in material specifications. Whenever possible, alternative test methods should be used, and their development is encouraged. This test method will not, in general, permit conclusions to be drawn concerning the relative arc resistance rankings of materials that may be subjected to other types of arcs: for example, high voltage at high currents, and low voltage at low or high currents (promoted by surges or by conducting contaminants) [1].

ASTM D495 states within itself that it should not be used in material specifications, indicating that the usage of insulators in these environments cannot be pre-determined and testing under specific

expected conditions must be done beforehand. These limitations severely reduce the applicability of the standard and any requirements derived from its results.

2.3 Insulator Pollution

UL 840 defines the safe distances for insulators based on the previously listed CTI values of the insulator, the level of pollution expected, and the applied voltages. UL 840 pollution degrees are based on the presence of contaminants and are listed as follows [4]:

Pollution Degree 1: No pollution or only dry, nonconductive pollution. The pollution has no influence.

Pollution Degree 2: Normally, only nonconductive pollution. However, a temporary conductivity caused by condensation may be expected.

Pollution Degree 3: Conductive pollution, or dry, nonconductive pollution that becomes conductive due to condensation that is expected.

Pollution Degree 4: Pollution that generates persistent conductivity through conductive dust or rain and snow.

UL 840 lists steps that can be taken to control the pollution degree of the system as part of the design considerations. From 6.4 – CONTROL OF POLLUTION DEGREE [4]:

Pollution Degree 1: achieved by the encapsulation or hermetic sealing of the product.

Pollution Degree 2: achieved by reducing possibilities of condensation or high humidity at the creepage distance, through the provision of ventilation or the continuous application of heat, using heaters or continuous energizing of the equipment when it is in use. Continuous energizing is considered to exist when the equipment is operated without interruption every day and 24 hours per day or when the equipment is operated with interruptions of a duration which do not permit

cooling to the point of condensation to occur.

Pollution Degree 3: achieved using appropriate enclosures which act to exclude or reduce environmental influence, particularly moisture in the form of water droplets.

The IEC technical specification IEC/TS 60815-1 [31] defines the selection and dimensioning of high-voltage insulators intended for use in polluted conditions. As with UL 840, IEC/TS 60815-1 identifies types of pollution, separated into Type A and Type B, as well as the evaluation of site pollution severity, which considers various environments and the pollutions expected under these conditions.

Table VII – Examples of typical environments for pollution severity [31]

Site Severity	Environment Example
Very Light (1)	>50km from the sea, a desert, or open dry land >10 km from man-made pollution sources
Light (2)	10-50 km from the sea, a desert, or open dry land 5-10 km from man-made pollution sources
Medium (3, 4)	3-10 km from the sea, a desert, or open dry land 1-5km from man-made pollution sources Or within "Light" range and: Dense fog occurring after dry pollution accumulation season And/or heavy rain with high conductivity And/or a high NSDD level, 5-10 times the ESDD
Heavy (5, 6)	Within 3 km of the sea, a desert, or open dry land Within 1 km of man-made pollution Or within "Medium" range and: Dense fog occurring after dry pollution accumulation season And/or heavy rain with high conductivity And/or a high NSDD level, 5-10 times the ESDD
Very Heavy (7)	Within "Heavy" range and: Directly subjected to sea-spray or dense saline fog Or directly subjected to contaminants with high conductivity, cement type dust with high density, and with frequent wetting by fog or drizzle Or Desert areas with fast accumulation of sand and salt along with regular condensation
Light to Heavy (8)	Within 3 km of the sea Within 1 km of man-made pollution sources Associated with the possibility of heavy sea-fog and/or industrial particulate fog

Type A pollution is defined as a solid pollution with non-soluble components deposited onto an insulator's surface, which becomes conductive when wetted. Type A pollution is best

characterized by Equivalent Salt Deposit Density (ESDD) / Non-Soluble Deposit Density (NSDD) measurements, which will be described later. Type A pollution is most often associated with inland, desert, or industrially polluted areas, but can also be found in coastal areas, where a dry salt layer builds on the surface and becomes wetted. Type A pollution is comprised of soluble pollution, which forms a conductive layer when wetted, and non-soluble pollution, which forms a binding layer for the soluble pollution [31].

Type B pollution occurs when liquid electrolytes are deposited on the insulator with little or no non-soluble components. Type B pollution is best characterized by conductance or leakage current measurements. Type B pollution is most often associated with coastal areas where salt water or conductive fog is deposited onto the insulator surface. Other type B pollution source examples are crop spraying, chemical mists, and acid rain [31].

Another distinction in types of pollution is based around the solubility of the pollutant, which determines how the pollutant is measured. This distinction is separated into soluble pollutants, typically salts of both low and high solubility, and non-soluble pollutants. Soluble pollutants are measured by determining the Equivalent Salt Deposit Density (ESDD) of the contaminants, whereas non-soluble pollutants are measured using Non-Soluble Deposit Density (NSDD). A plot describing the relationship of ESDD and NSDD to pollution level is shown in Figure 8.

The ESDD of an objects surface pollution is used to describe the level of contamination of an object based on the equivalent amount of NaCl salt deposit. ESDD is measured in mg/cm^2, and it can be defined as the equivalent mass of dissolved salt in the wet pollution layer per unit area of the insulator. The NSDD of an objects surface pollution is similar to the ESDD except that the

pollutants are non-soluble such as clay, dust, or metal shavings. NSDD is also measured in mg/cm^2 and is the mass of deposited non-soluble pollutants per unit area of the insulator.

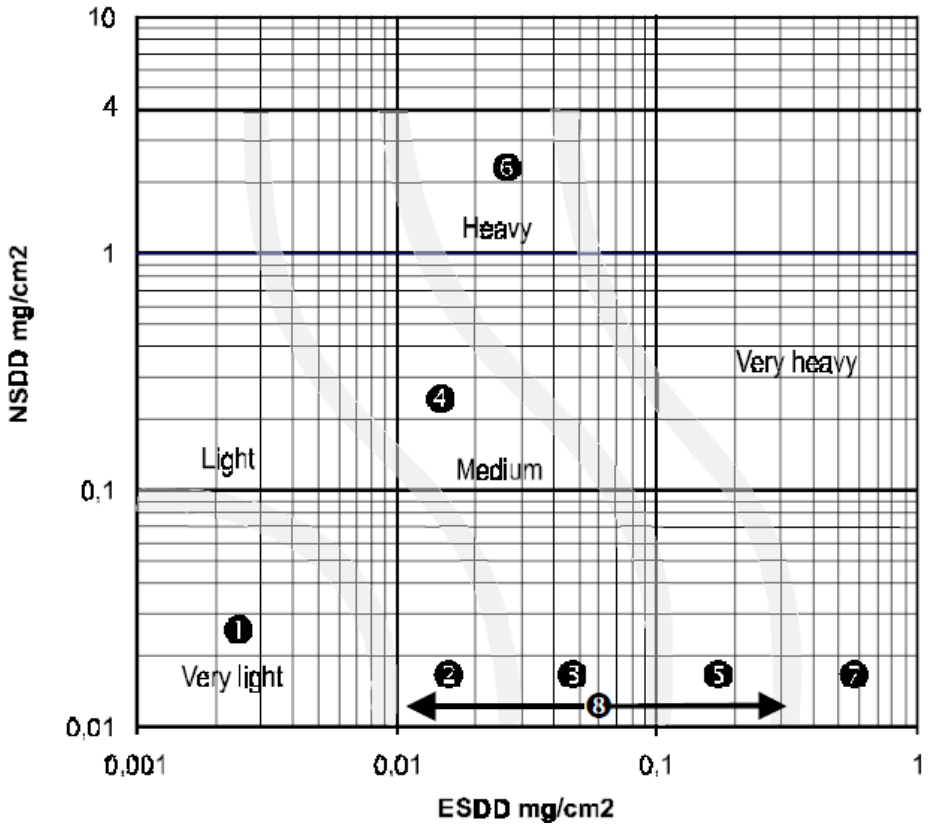

Figure 8 – Relation between ESDD/NSDD and pollution severity [31]

The following steps for ESDD and NSDD pollution collection are adapted from IEC/TS 60815-1 [31], where they are defined for pollution measurements on insulators used in transmission lines. The basic pre-requirements for pollution collection for measurements of both ESDD and NSDD are the same: the surfaces of the insulator should not be touched to avoid the loss of any pollution material, surgical gloves must be worn while handling the insulator, and the measuring container must be cleaned prior to use to remove any potential contaminants or previous pollution residue.

The washing technique for pollution collection from the surface of an insulator requires the insulator sample to be placed in a bowl with distilled water, and the surface of the insulator is to be gently wiped with the gloved hand to remove the pollution from the surface and into the bowl. The polluted solution is poured into a labelling container and should be gently stirred; high solubility pollutants should be stirred for a short period of time, approximately 5 minutes, to ensure a complete solution, whereas lower solubility pollutants should be stirred for 30-40 minutes [31].

The determinations of the ESDD and NSDD of the pollutant(s) are performed separately. To calculate the ESDD, the temperature and conductivity of the polluted solution must be measured. The following formula is used to provide a conductivity correction for temperature [31, 50]

$$\sigma_{20} = \sigma_{\theta} [1 - b(\theta - 20)] \quad (2)$$

where:

θ is the solution temperature (C)

σ_{θ} is the volume conductivity at temperature of θ (S/m)

σ_{20} is the volume conductivity at temperature of 20 ºC (S/m)

b is a factor dependent on temperature θ, and is obtained by the formula:

$$b = -3.200\, x\, 10^{-8}\, \theta^3 + 1.032\, x\, 10^{-5}\, \theta^2 - 8.272\, x\, 10^{-4}\, \theta + 3.544\, x\, 10^{-2} \quad (3)$$

From σ_{20} the ESDD from the surface of the polluted insulator is calculated by the formulas:

$$Sa = (5.7 * \sigma_{20})^{1.03} \quad (4)$$

$$ESDD = Sa * V/A \quad (5)$$

where:

V is the volume of distilled water used (cm^3)

A is the surface area of the insulator where pollution was collected (cm^2).

Once the ESDD of the solution has been measured, the water is poured through a pre-dried and weighed filter of grade GF/A 1.6 µm. The filter paper catches and retains the pollutants from the solution as it is poured through. It is then dried, evaporating the water and leaving behind the pollutants, and weighed again to determine the mass of the remaining residue, the NSDD. The NSDD measurement procedure is shown in Figure 9. The NSDD is then calculated by the formula

$$NSDD = 1000(W_f - W_i)/A \quad (6)$$

where:

W_f is the mass of the dried filter paper with pollutants (g)

W_i is the initial mass of the dried filter paper (g)

A is the surface area of the insulator where pollution was collected (cm^2).

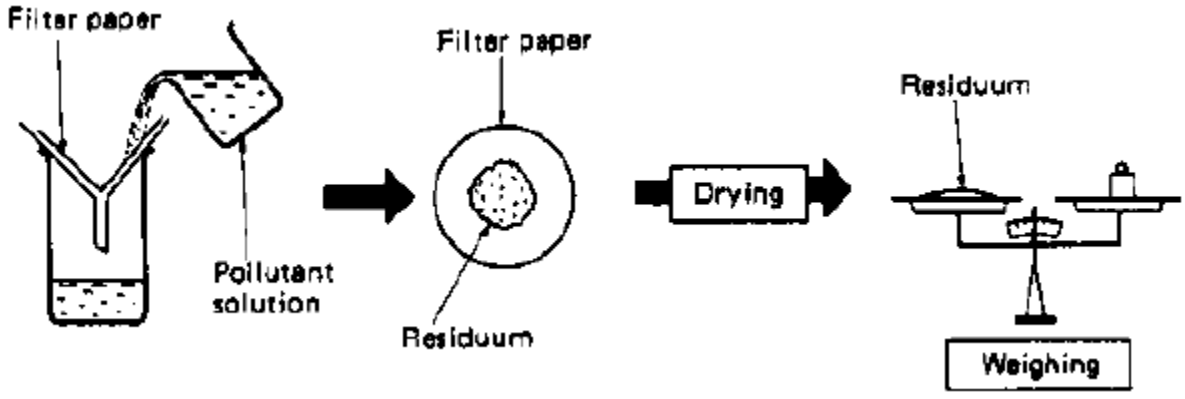

Figure 9 – Procedure for measuring NSDD [31]

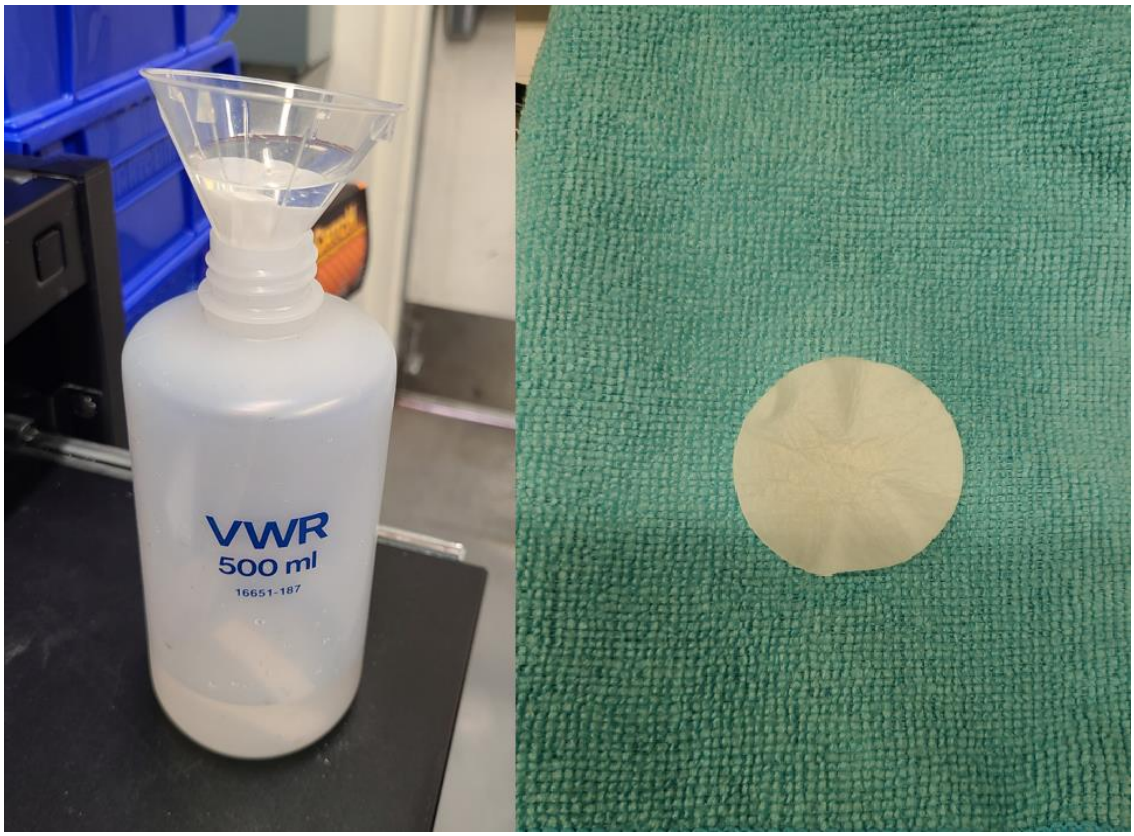

Figure 10 – Solution pouring through funnel and filter (left), filter drying with pollutants (right)

Above, in Figure 10, the first two steps of the NSDD measurement process are displayed. The ESDD and NSDD measurement processes are used as part of the pollution application procedure to determine the levels of the various pollutants and ensure a consistent level of application. These measurements are also used in the development of pollution application procedures for the pollutants which do not have established methods.

CHAPTER III

EXPERIMENTAL SETUP

In the experiments performed here, two different experimental setups were used to apply high electric fields continuously and transiently. The bulk of the study was performed applying continuous high electric fields using a high voltage potential tester (hi-pot tester). Samples found to have a surface flashover potential less than 12 kV under continuously applied electric fields were then studied transiently. A test bench was designed that incorporates flat copper rails that are adjustable, such that the gap between them can be altered for studying samples of differing widths. The samples are held snugly in place to maintain consistent contact along each side of the sample while under test. Flat copper rails are used to minimize any electric field enhancements that could alter the surface flashover potential.

3.1 DC Testing – Hi-pot Tester

A Hi-pot tester is a voltage source that slowly applies increasing voltage until a pre-determined, very low, amount of current flow is measured. The supply typically has adjustable peak voltages, ramp rates, and dwell time settings, among others. In the studies performed here a HIPOTRONICS AC/DC D149-DI Test System capable of supplying up to 100 kVAC at 60 Hz and 100 kVDC was used. The breakdown current threshold can be set as low as 0.1 mA and has a breakdown detection time within 10 μs. A photograph of the hi-pot tester is shown in Figure 11. The leads from the hi-pot tester are attached to the test setup, shown later, using banana jacks, and the sample is placed in the chamber as shown in the upper right photo of Figure 11. Once the sample is secured in place, the tester slowly applies increasing voltage across the two rails at an adjustable rate between 0.1 – 10 kV/s. The hi-pot tester considers a breakdown event by measuring the current passing between the electrodes; once the current surpasses a user-preset threshold, the

test is stopped, and the voltage is recorded. Each test was performed three times for each type of sample, and the average was recorded. Experiments were performed with applied voltages as high as 60 kVDC.

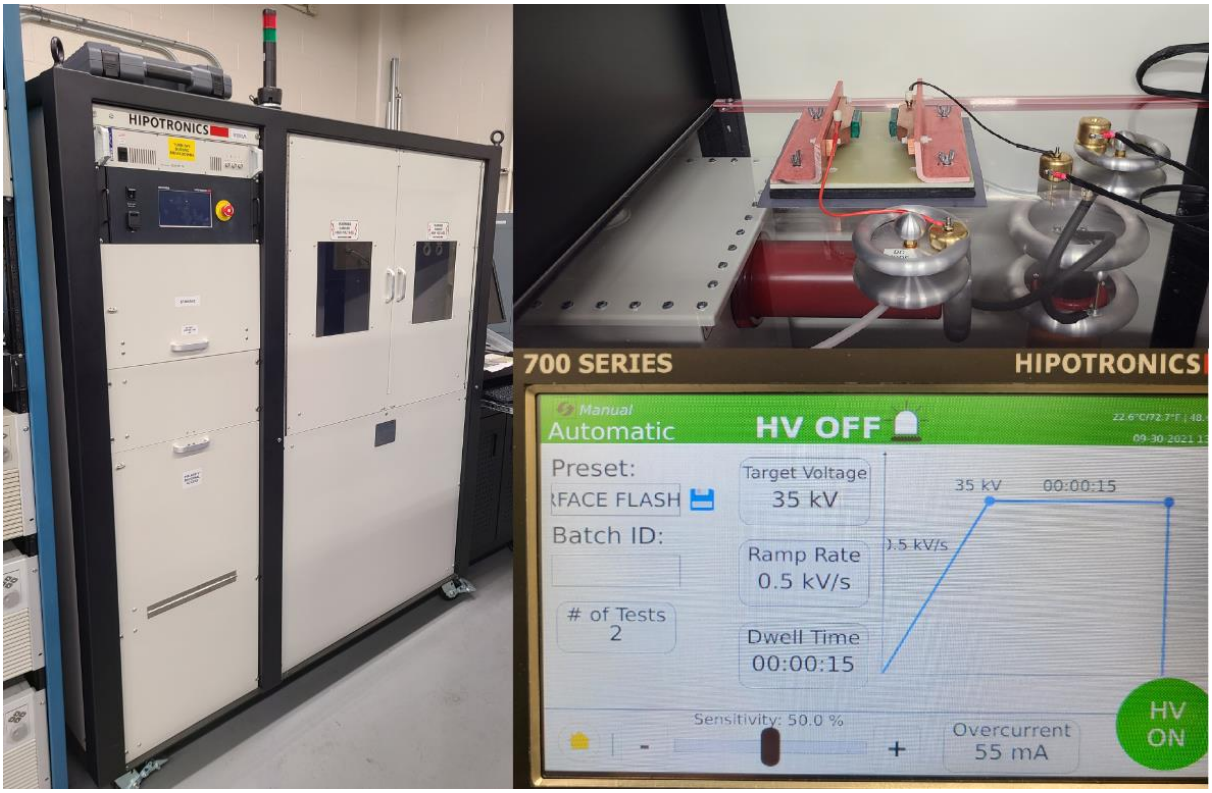

Figure 11 – HIPOTRONICS Hi-pot tester (left), internal cabinet (upper right), test controls (lower right)

3.1.1 Test-bench 1

A few different variations of the electrode/sample setup, referred to as the test-bench, were used. The first consisted of two 1.5” x 0.5” x 8” copper rails mounted to fiberglass “L” brackets, shown in Figure 12. The brackets were bolted to a piece of 12” x 12” x 0.5” G10 that is slotted to allow for the brackets to slide inwards towards each other, or outwards away from each other, depending on the width of the insulator being tested. The sample is placed on the edges of ceramic blocks to elevate and support the sample, while the fiberglass-mounted copper plates provided clamping pressure to the sample. The copper bars were lightly sanded on the edges, though no

other modifications were performed. The sample is kept well inside the flat section of the rails and is lifted towards the middle of the copper surface area using ceramic blocks; this aims to minimize any edge effects. The copper surface was covered with a polyester/silicone single coated splicing tape everywhere except around the surface exposed to the sample. Though it is not expected that the tape will prevent breakdown through it, the aim was to force the exposed copper only to the sample region of interest.

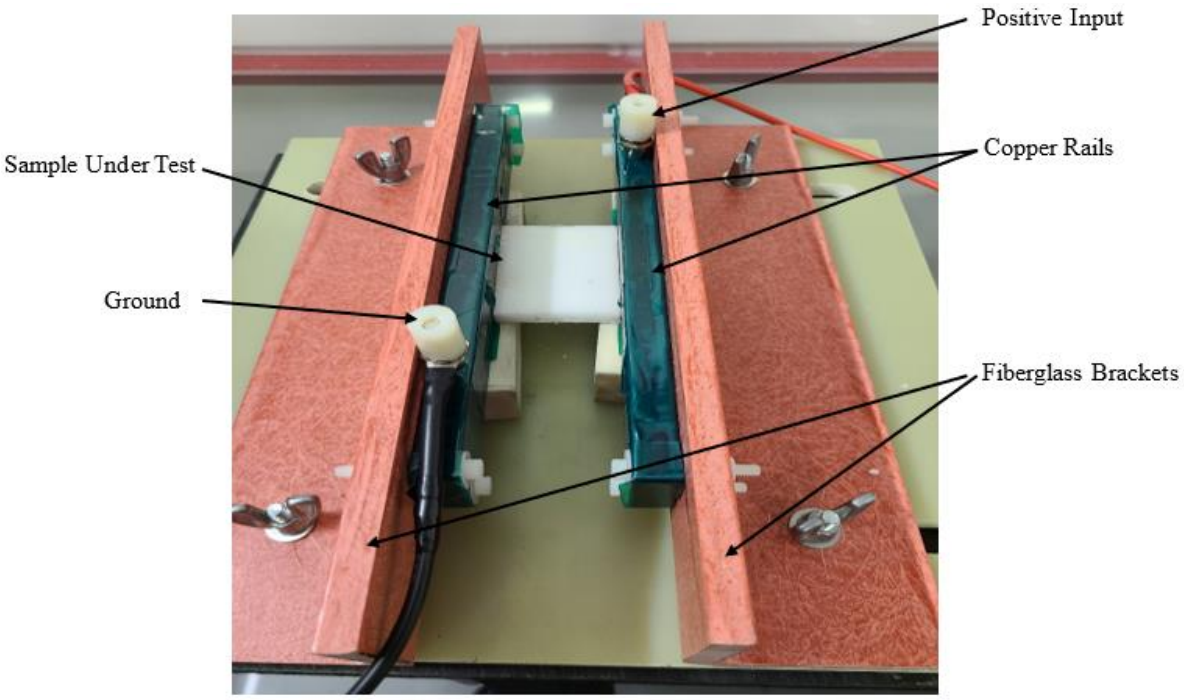

Figure 12 – Test-bench 1 for hi-pot tester

When using the first test bench design, there were some consistency issues observed during testing. As discussed, the copper rails extend well beyond the sample under test in both directions, as shown above in Figure 12. Breakdowns were often experienced outside of the sample test region, particularly at the corners of the copper rails where the charge density is highest. The breakdown often occurred through the polyester/silicone tape used to limit field exposure outside of the insulator surface region. To mitigate this, a revised design was implemented.

3.1.2 Test-bench 2

In the second test bench design, seen in Figure 13, the copper rail was designed to be shorter than the samples to reduce the clearance breakdowns on the edge of the sample away from the surface flashover test region. Secondly, the copper bars mounted to the angled frames were recessed to further reduce the likelihood of undesired breakdowns which occurred at the edges near the mounting bolts. The rails were designed as two pieces so that the surface exposed to the sample can be quickly and easily replaced, seen in Figure 14, during the high energy transient breakdown experiments described later. This design fits within the constraints of the metal structure used to house the setup in the higher energy testing shown later. In operation these improvements significantly reduced unwanted breakdowns, producing more accurate breakdown results.

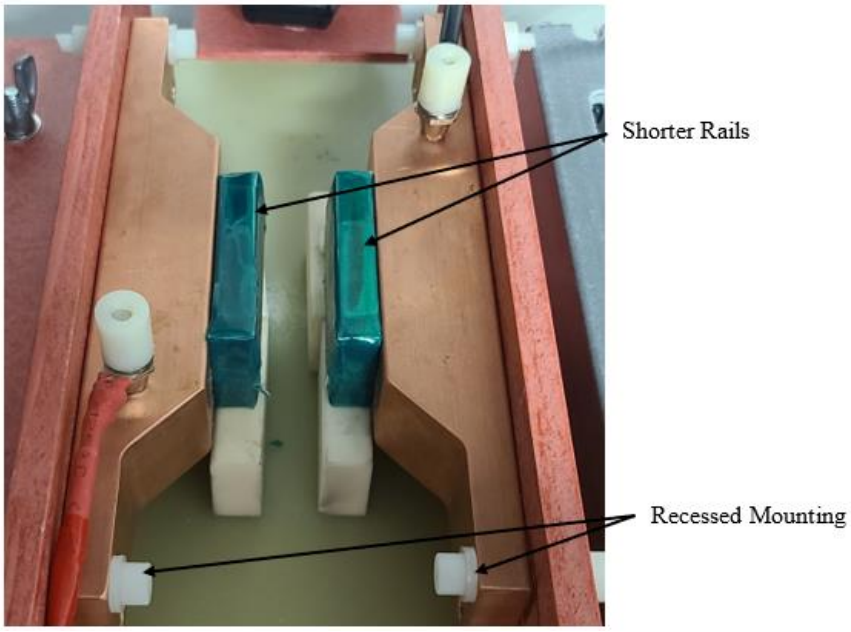

Figure 13 – Test-bench 2

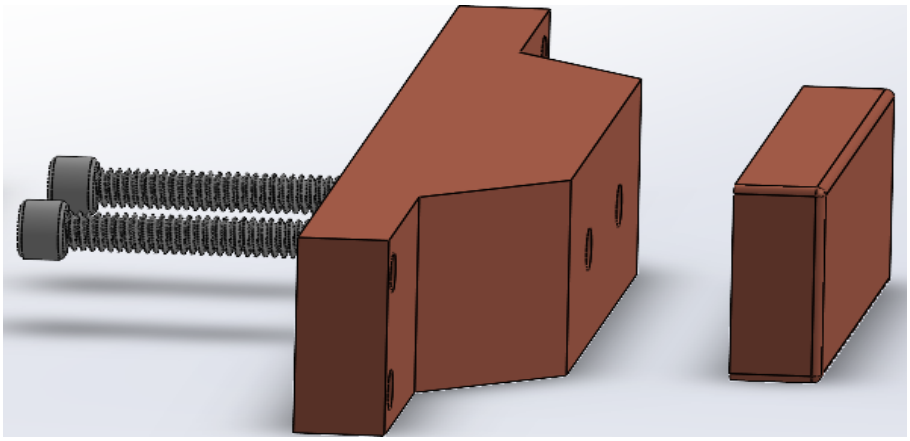

Figure 14 – Two-piece rail design

3.2 Pulsed Power Testing – Higher Energy Transient Voltage Experiments

A goal of this part of the work is to measure variation observed in the surface flashover potential when it is applied under a slowly ramping DC voltage and again when it is applied all at once as a transient waveform to the sample under test. In the latter experiments voltage is applied using two 11 kV, 826 μF capacitors connected in parallel that serve as the primary energy store. The capacitors are part of a larger 1 MJ pulsed power supply that was initially used as a railgun power supply in the early 1990s. Each 1 MJ pulsed power supply has 22 capacitors that are charged in parallel and then discharged through a triggered spark-gap switch into a 33 μH inductor. A crowbar diode array is present to allow the inductive energy to flow in the circuit once the load is engaged. A graphical representation of a module is shown in Figure 15, a simple circuit schematic of a module is shown in Figure 16, and a photograph of all five modules in place in the laboratory is shown in Figure 17.

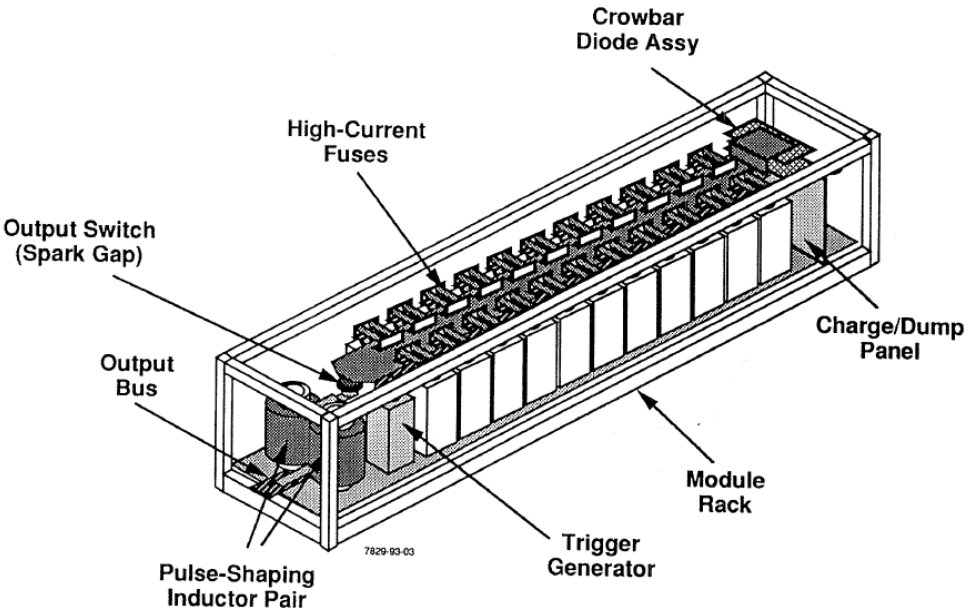

Figure 15 – Simple graphical representation of a 1 MJ pulsed power supply module

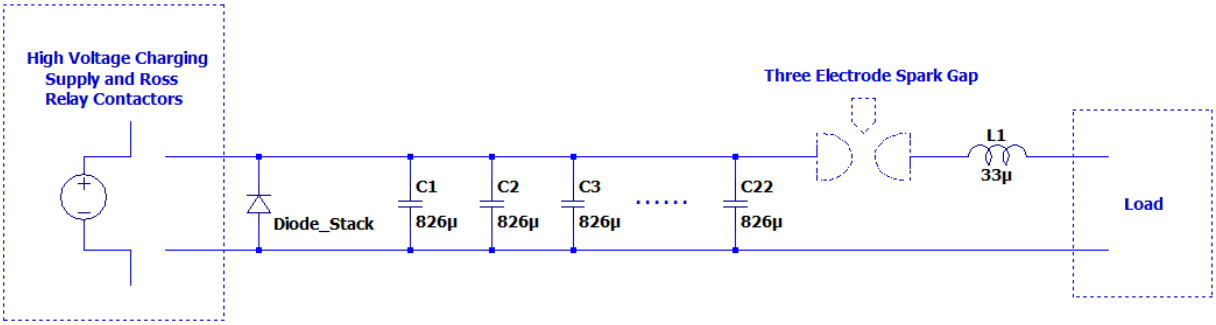

Figure 16 – Simple schematic of a 1 MJ pulsed power module

Figure 17 – Pulsed power supply capable of 1 MJ at 11 kV. 100 kJ at 11 kV operational

In the experiments performed here, 1 MJ of energy would be extremely excessive. Therefore, the fuses that connect 20 of the 22 capacitors to the positive charging bus were disconnected, isolating them from the circuit. This left two capacitors were kept in the circuit as shown schematically in Figure 18. The output of the module is connected to high current feed plates using high voltage MCM350 coaxial cable. The copper feed plates used to serve as the breech of a low power railgun and can conduct just over 1 MA, seen in Figure 19. Even though 20 of the capacitors have been removed, there is still the potential for over 100 kJ of energy to be dissipated in the surface flashover arc if the capacitors are fully charged. This is a significant amount of energy and therefore the load test section must be sufficiently contained. To achieve this, thick steel containments previously used to house a small caliber railgun are used. The setup allows for a sufficient compressive force to be placed on the test setup such that the repulsive forces and arc blast pressure are contained. A solid model of the test setup along with several photographs are shown in Figure 20 and Figure 21. The containments are fabricated in 1 m long sections that are placed in series with each other when used as a railgun containment. In these experiments, only the first 1 m long section is used as shown in Figure 21.

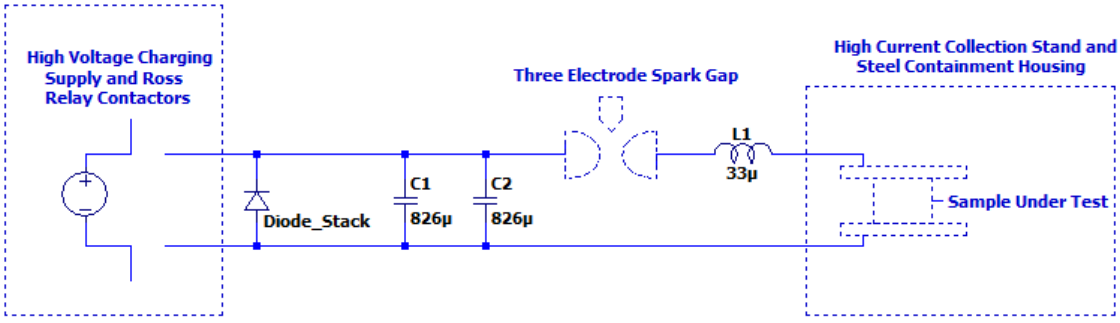

Figure 18 – Final high-energy circuit schematic used to apply high-voltage transients to the samples under test

Figure 19 – Photograph of the high-current collection plates used to conduct current from the pulsed power supply into the flashover test setup

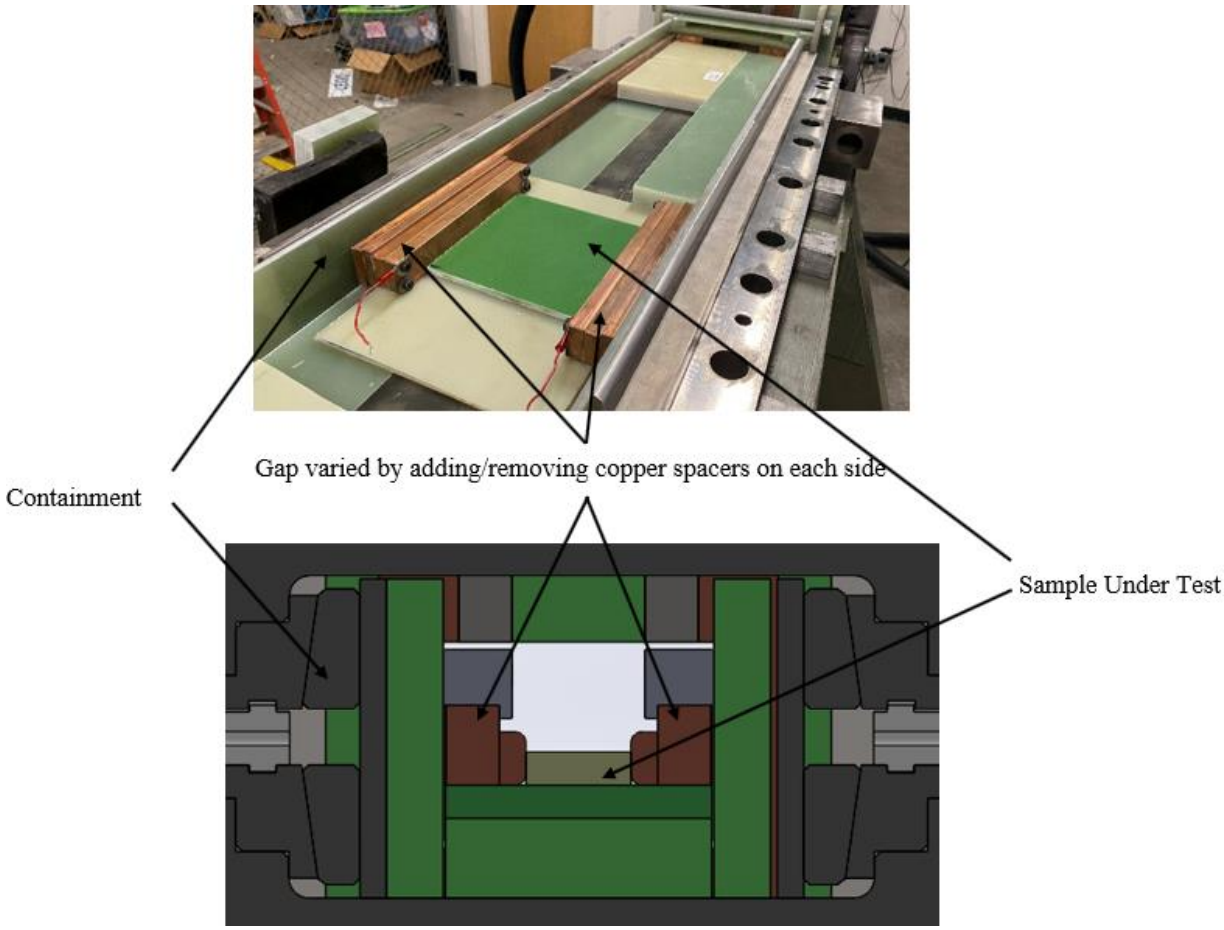

Figure 20 – Overhead view of insulator test section (top) and breech view image for detail (bottom)

Figure 21 – Photograph of the 1 m section of the railgun testbench

The first round of experiments was performed using a test setup shown in Figure 20, identical to test bench 1 shown earlier. When continuously applied the spark gap was short circuited, and the charge voltage was ramped up in 500 V increments up to 9 kV. When pulsed the spark gap was connected, the capacitive storage was charged, and the voltage was applied by triggering the spark gap.

The transient voltage test bench centers around two copper rails, one charged positive and one negative. The sample is placed between these two rails, and depending on the creepage distance being tested, numerous copper spacers can be placed to alter the distance between the electrodes. The rails and sample are housed within a steel containment assembly. To ensure longitudinal strength and electrical isolation of the system, the rails lie on a one-inch-thick slab of G10, with a second slab placed on top. Two steel spacers are placed on either side of the rails, with a G10 spacer between the copper and steel; the G10 serves as an insulator between the copper and steel. Each rail is connected by a copper spacer to two shorter copper rails. At the breech, each of these rails is secured to a thin copper plate by two steel clamps. These plates are to ensure a strong connection between the rails and the coaxial cables, thus preventing arcing. The sample is then

press fit between the two copper rails. Two G10 slabs are placed on top of the rails and the upper half of the steel containment assembly is placed on testbed to ensure the system is electrically isolated and structurally supportive enough to handle the stress of the magnetic force.

As before with the first testbench used in the hi-pot tester, the first test configuration for the pulsed power testing experienced difficulties. One of note centered on the mounting hardware for the copper rails; the mounting stud and nut protruded into the surface test space leading to early breakdowns occurring before surface flashover was induced. These breakdowns happened through the Polyester/Silicone tape and are highlighted in Figure 22.

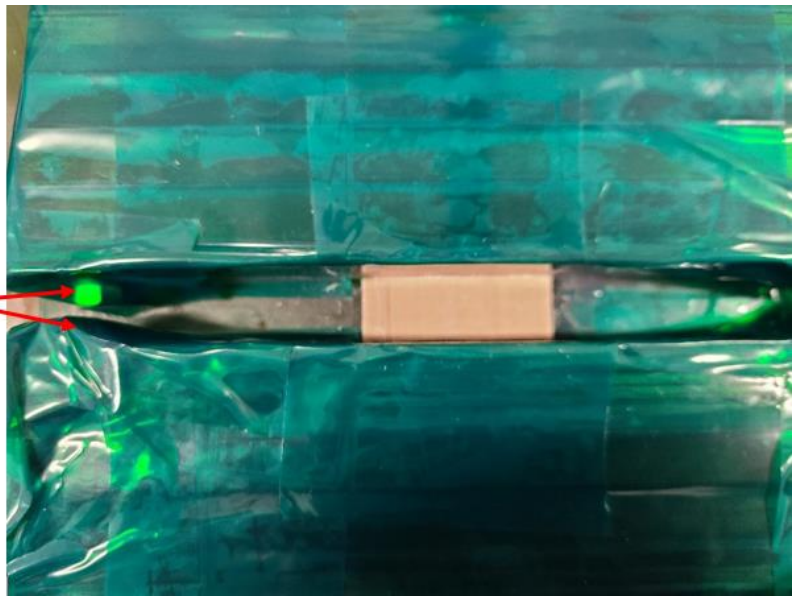

Figure 22 – Sample under test in pulsed-power testbench

As the pulsed power testing involves a high level of energy for the breakdowns, when a breakdown does occur the copper rails and mounting hardware are damage or destroyed, as seen in Figure 23. It is these considerations that led to the implementation of the two-piece rail design from the hi-pot test stand into the pulsed power test stand.

Figure 23 – Copper rails damaged by breakdown

3.2.1 Implementation of New Rail Design

The implementation of the two-piece rail design reduces likelihood of early breakdown outside of the insulator surface. As the breakdown surface of the two-piece design is easily removable, when a breakdown occurs the electrode can be replaced more quickly while also using less material. As before, the distance between rails is adjusted by adding or subtracting copper rail spacers of various thickness to reach the desired distance for the sample under test. The new rail design as installed on the pulsed power testbench is shown below in Figure 24, and spent copper test samples are shown in Figure 25.

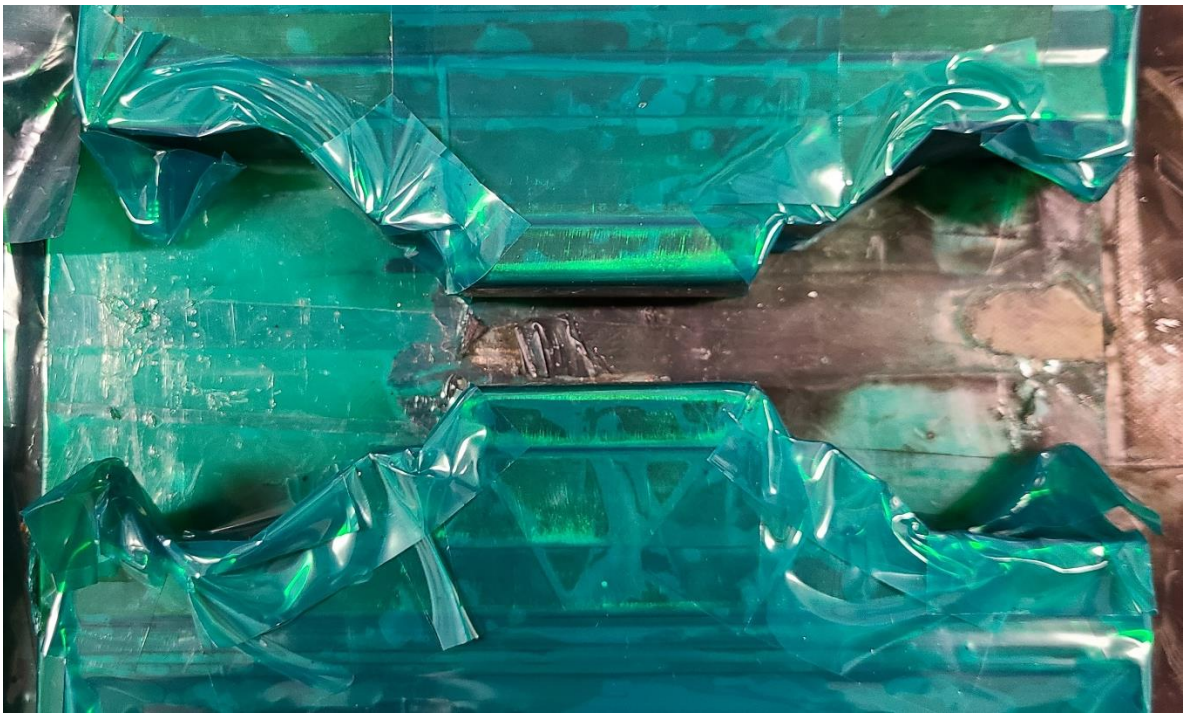

Figure 24 – Two-piece rail design as installed on pulsed power testbench

Figure 25 – Two-piece design electrodes after a breakdown

CHAPTER IV

EXPERIMENTAL PREPARATION AND PROCEDURE

The samples were prepared from the five previously listed insulator materials of G9, G10, G11, Delrin®, and polycarbonate in three sizes: 18.5 ± 0.5 mm, 43.5 ± 0.5 mm, and 75 ± 0.5 mm. The sizes were so chosen as they occur in the UL 840 standard as part of the creepage distance requirements correlating with listed AC rms and DC breakdown voltages; the UL 840 creepage distance requirements do allow for interpolation of both voltage and distance values for accurate determination. During preliminary testing, it was noted that the breakdown voltages of the 75 ± 0.5 mm samples exceeded 60 kV; as the intent is to test surface flashover at MVDC and pulsed power conditions of less than 20 kV the 75 ± 0.5 mm samples were not tested further. The samples were cut using a water jet cutter, each from single sheets of each material to ensure consistency in the comparative tracking index (CTI) of each sample tested at each level of pollution. This also allows for the non-polluted samples to be used as a baseline of the surface flashover voltage requirements for comparison with the polluted samples. The edges of the cut samples were then lightly sanded with 400 grit sandpaper to remove any burrs or other inconsistencies. Finally, the samples were wiped with a lint-free microfiber cloth and isopropyl alcohol to remove any dust, oils, and residues left behind.

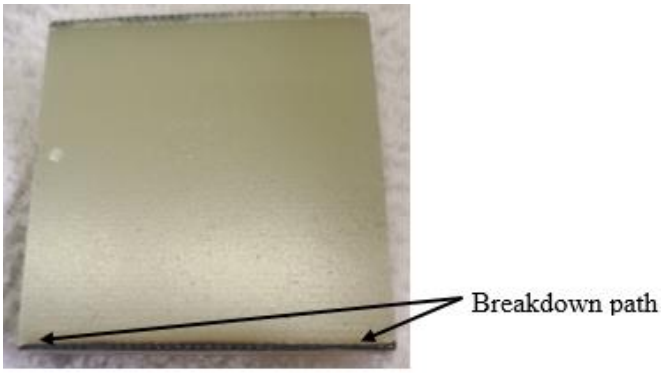

Figure 26 – Sample with surface lip that allowed for current to pass (edge tracking)

4.1 Pollutants and Application

The pollutants selected for testing followed both the standards investigated as well as the application, such as pollutants that might be found in a shipboard environment. Kaolin clay was tested, as it is listed as an inert material used to improve the adherence of pollutants to insulator surfaces [51], the veracity of which was examined. The kaolin clay is expected to perform as a UL 840 Pollution Degree 1 – dry, nonconductive pollution that has no influence on the breakdown.

Pollution levels 2 and 3 introduce uncertainty into the characterization of contaminants. Pollution degree 2 is listed as nonconductive pollution where a temporary conductivity by condensation may be expected, while pollution degree 3 is defined as conductive pollution or dry nonconductive pollution that becomes conductive due to condensation. The overlap between pollution levels occurs when condensation is applied, as the definition of a temporary conductivity is indistinct. Three pollutants were selected to fit the testing requirements for pollution levels 2 and 3: carbon dust, calcium sulfate ($CaSO_4$) salt, and sodium chloride (NaCl) sea-salt. The pollutants were selected for their expected conductivity as well as their likely presence in shipboard environments. Carbon dust, in the form of soot, can be generated as a byproduct of the incomplete burning of organic matter, such as the exhaust of diesel generators. Calcium sulfate is a type of low solubility salt commonly found in precipitation [52]. Sea-salt can be found on components because of sea-spray or salt fog leaving behind trace amounts in the surface residue.

The iron powder was selected for the second round of testing to meet the UL 840 Pollution Degree 4 – pollution that generates persistent conductivity through conductive dust. The iron powder is continuously conductive and can be found in environments where friction between metallic components is present.

Pollutants were applied to the insulators using methods documented in applicable standards when available; when application standards are not available pollutant application is performed to best produce consistent and repeatable pollution to the insulators. All pollutant application was conducted to ensure a level of pollution tolerance of ± 15% as defined in IEC 60507 [50].

4.1.1 Salt-fog Pollution – NaCl

Clean samples were polluted with a surface layer of sea salt using a custom salt-spray chamber. The chamber consists of a large acrylic box with a sealed lid with a pressure vent. An atomizing spray nozzle is connected to an air compressor, and the saltwater solution is poured into the liquid inlet; when combined in the nozzle a fine mist is produced and sprayed throughout the chamber.

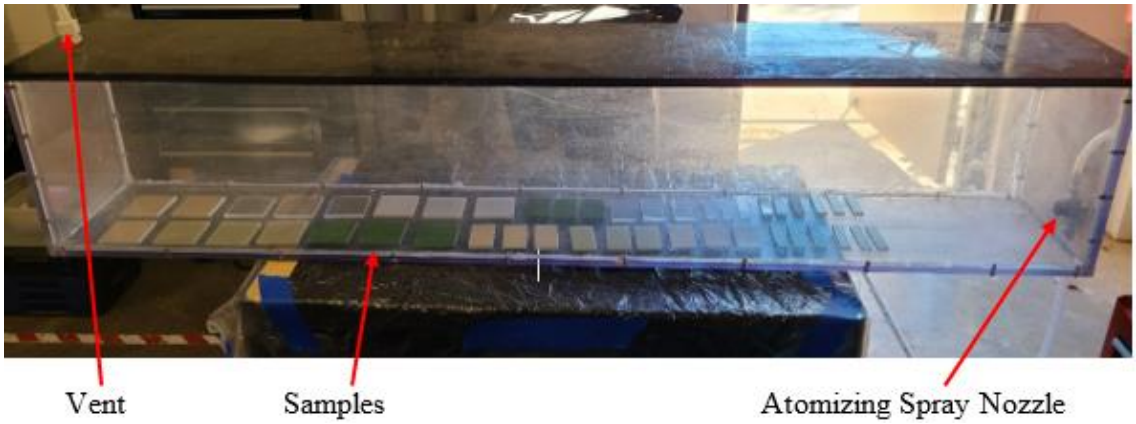

Figure 27 – Salt-spray chamber

A one-liter seawater solution is created by mixing 40 g of ASTM D 1141-52 Formula A 'SEA-SALT' with distilled water; the measured sea-salt formula is placed in a container and the water is added until one liter of total solution is reached. The solution is stirred until completely mixed with no solids remaining. This creates a solution of 4% salinity which meets the standards set forth [50, 51].

The solution is uniformly sprayed into the chamber with the atomizing inlet air pressure maintaining 40psi; this pressure was determined empirically to produce a fine, steady spray throughout the chamber, seen in Figure 28. The spraying process with one liter of solution takes approximately 20 minutes, during which each sample becomes fully coated in the solution as the mist passes through the chamber from the nozzle to the vent.

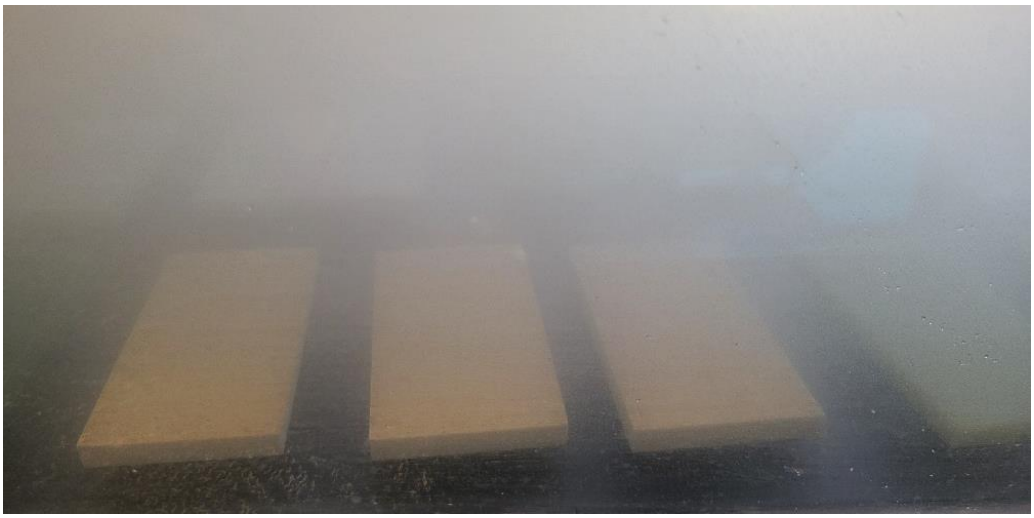

Figure 28 – Sample undergoing salt-spray

After the spraying is complete the samples are taken out of the chamber and placed on clean terrycloth towels to dry, seen in Figure 29, for a minimum of 18 hours in accordance with IEC 60507 [50] which states that natural drying of the pollution layer on an insulator is sufficient provided that the drying period exceeds 8 hours. Once the samples are dry, a fine layer of salt residue is left behind on the surface and the samples are ready for testing.

Figure 29 – NaCl polluted samples drying

After the sea-salt polluted samples underwent testing, three samples were randomly selected to determine the ESDD of the samples using the method described in section 2.3 – Insulator Pollution. To measure the volume conductivity of the solution, a liquid resistor was fabricated using the solution as the electrolyte. The liquid resistors were constructed using plastic tubing with flat aluminum electrodes inserted into each end with the solution filling the space between. The resistor was connected between the nodes of a DC power supply and the voltage was swept between 40 and 120 VDC. Using the voltage and current output measurements of the DC power supply the resistance was calculated and the average of all the measurement points was used with the distance between the electrodes to determine the volume conductivity σ_θ for the ESDD calculations.

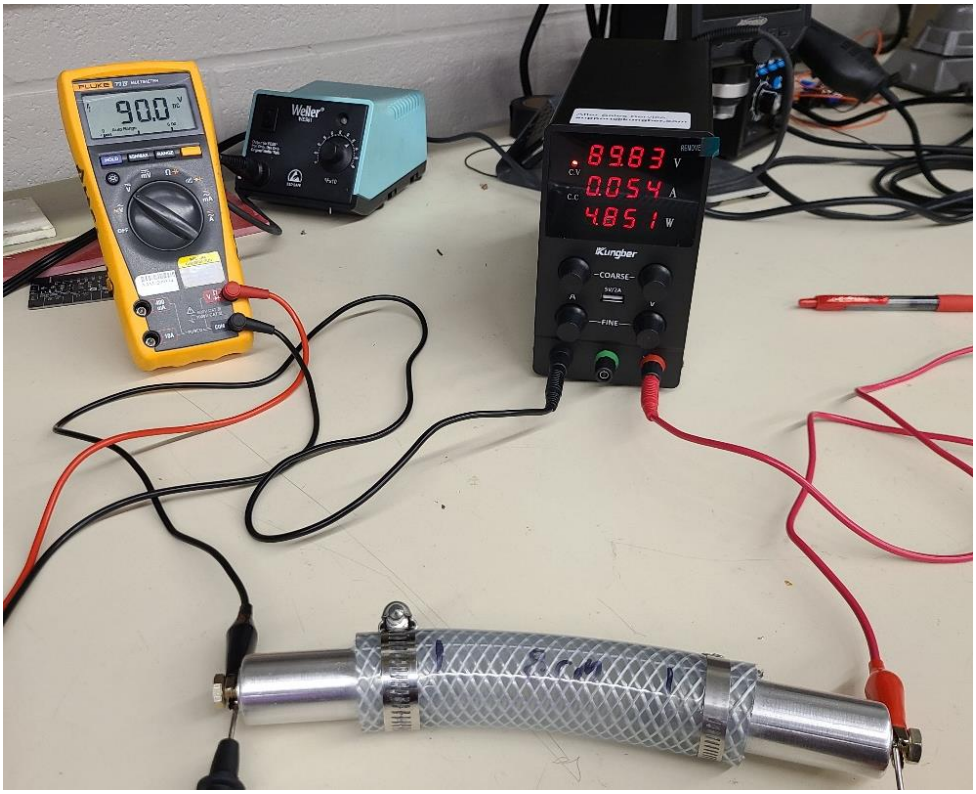

Figure 30 – Liquid resistor for sea-salt solution ESDD testing

Table VIII – NaCl solution resistance results

Voltage (V)	Current (A)	Resistance (Ω)
40.00	0.020	2000
50.00	0.026	1923
60.00	0.031	1935
75.00	0.040	1875
90.00	0.053	1698
100.0	0.061	1639
120.0	0.079	1519

From the NaCl solution resistance testing, an average resistance of 1798 Ω was calculated across the range from 40 to 120 V. The surface pollution from three of the 75 mm x 75 mm samples was used to ensure a measurable solution was produced (area A = 168.75 cm^2), giving an average across multiple samples, with the results being used to determine the average sea-salt pollution per sample. The temperature of the NaCl solution (θ) measured to 24.2 ºC before and after testing. The volume (V) of the water resistor measured out to 42.5 cm^3, producing a volume conductivity (σ_θ)

of 0.0070 S/m. Inserting these measurements into the ESDD measurement and calculation formulas produces

$$b = -3.200\ x\ 10^{-8}\ 24.2^3 + 1.032\ x\ 10^{-5}\ 24.2^2 - 8.272\ x\ 10^{-4}\ 24.2 + 3.544\ x\ 10^{-2}$$

giving $b = 0.0210$, which then determines

$$\sigma_{20} = 0.0070\ S/m\ [1 - 0.00210(24.2 - 20)]\ .$$

With the adjusted volume conductivity of the solution σ_{20} = 0.0063 S/m, the salinity of the solution (*Sa*, kg/m^3*)* is calculated using

$$Sa = (5.7 * 0.0063\ S/m)^{1.03}.$$

Finally, the ESDD of the solution is calculated with

$$ESDD = 0.0327\ {}^{kg}/_{m^3} * \frac{42.5cm^3}{168.75cm^2}$$

which gives an average ESDD of 0.0082 mg/cm^2 across the three samples measured.

While there is minimal information available on measured pollution levels on insulators in shipboard environments, significant material is available on the pollution and testing of power station systems. Testing conducted at the Big Eddy Substation test center in Oregon performed laboratory pollution tests of 0.02 – 0.2 mg NaCl/cm^2; and they noted that the natural pollution that occurred at HVDC stations measured considerably lower, typically around 0.003 mg NaCl/cm^2 after 12 – 18 months [53]. Testing of composite power network insulators used in China calculated average values of the ESDD of the upper surface of insulators to fall within the range of 0.0128 mg/cm^2 to 0.0141 mg/cm^2 after 4 years of service [54]. The measured ESDD of the NaCl polluted samples falls within the range of the measured, naturally occurring pollution on HVDC stations

after 12 – 18 months and that of the higher level of pollution applied for testing and the development of maintenance guidelines for HVDC stations, while also near the average ESDD of HVDC insulators after 4 years of service, a range that shipboard environments can be reasonably assumed to fall within.

4.1.2 Non-soluble Salt Pollution – $CaSO_4$

Calcium sulfate ($CaSO_4$, aka Gypsum) is pollutant commonly found as a byproduct of evaporated rainwater [52]. In surface flashover testing of high-voltage insulators calcium sulfate is used in laboratory environments to simulate natural pollution conditions [54]. It is therefore being used here to simulate natural conditions for the medium-voltage and pulsed power testing environments.

Pure, food-grade calcium sulfate by Pure Ingredients Ltd. was applied to the samples by use of a shaker bottle. The powder was poured into the bottle, with the samples being dropped in individually prior to each test. The bottle was shaken for 10 seconds, after which the sample was carefully removed and handled using vinyl gloves to reduce pollution lost from the surface as well as reduce the possibility of any additional contaminants being introduced. A photograph is shown in Figure 31.

Figure 31 – Gypsum dusted sample after testing

Determination of the ESDD of the calcium sulfate pollution is achieved the same as it was for the sea-water pollution, as previously described. In the high-voltage environment testing, it was determined that $CaSO_4$ pollution builds on the surface of the insulator at a rate of ~2:1 as the NaCl pollution [28, 54], which was considered during the pollution application for $CaSO_4$. Using the same calculations as before, the average ESDD of the calcium sulfate pollution across three samples was measured to be 0.0210 mg/cm^2 for a ratio of ~2.5:1 compared to NaCl testing.

4.1.3 Metal Powder Pollution – Fe

Metal powder and shavings can be found in any environment where there is metal on metal friction and this is common in a shipboard environment, for example, around electromagnetic aircraft launch systems (EMALS). As the pollution cannot be completely contained, it can spread to other insulators or power systems and interfere with surface insulators. It is this commonplace occurrence that make it a pollutant to investigate and test. Iron powder was selected to simulate these conditions.

During preliminary testing it was noted that the iron powder did not stick to the clean insulator surfaces by any of the previously documented application methods. Reviewing test procedures for high-voltage insulators it is documented that an application of a base layer of kaolin clay, an inert pollutant, can be used to improve adherence of pollutants [50, 51].

Like the application of calcium sulfate, the shaker method was used to apply the base layer of kaolin clay before the iron powder was applied, seen in Figure 32. The insulator sample was then placed into the test bench and, using a measured lab scoop, 0.4 ± 0.04 mg/cm^2 of iron powder was sprinkled evenly across the surface of the insulator for the 18.5 mm samples and 1.0 ± 0.10 mg/cm^2 on the 43 mm samples. The amount of pollutant applied to the surface of the insulator was measured using the NSDD procedure listed underneath section 2.3 – Insulator Pollution

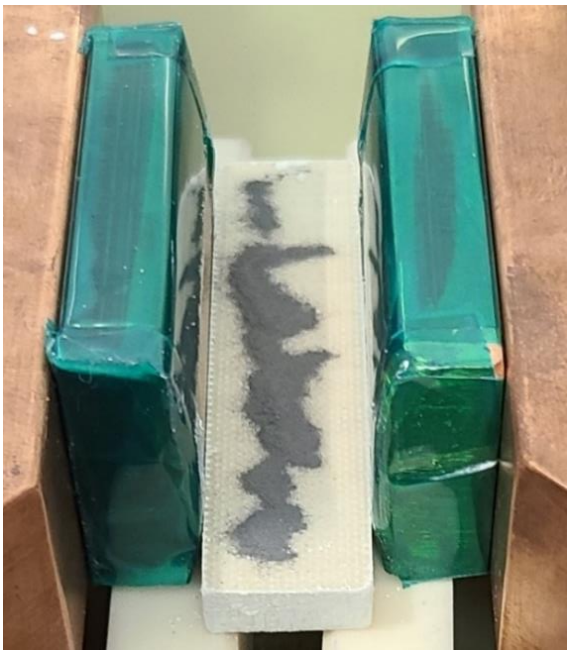

Figure 32 – Iron powder dusted sample prior to testing

4.1.4 Carbon Dust Pollution (Round 1)

In the first round of testing, the dry pollution of choice selected was a carbon dust that was applied via a shaker bottle. A container weas partially filled with the carbon dust pollutant and the sample was dropped into the bottle. The lid was securely fastened, and the bottle was shaken for 30 seconds to ensure a solid application of carbon dust. The sample was removed using a gloved hand reduce the inclusion of other pollutants as well as reduce the loss of applied carbon dust. A carbon coated sample is shown below in Figure 33.

Figure 33 – Carbon dust coated sample after testing

4.1.5 Kaolin Clay Pollution (Round 1)

Like the carbon dust pollution, the kaolin clay pollution was applied to the insulator material using the shaker bottle method. The container was partially filled with kaolin clay and the sample was dropped into the bottle, which was shaken for 30 seconds. The sample was removed using a gloved hand reduce the inclusion of other pollutants as well as reduce the loss of applied clay. A clay coated sample is shown below in Figure 34.

Figure 34 – Kaolin clay coated sample

4.2 Experimental Procedure

The samples were tested under the two environments discussed in Chapter III, using the DC hi-pot tester and the pulsed power test stand. The DC hi-pot tester was used to set a baseline for the samples under the various pollution conditions, primarily due to its ease of use and high accuracy for detecting low threshold current flow. The breakdown conditions of the samples in the DC tester were documented and used to determine which polluted samples to test in the pulsed power test stand.

Insulator samples were produced such that each level of pollution could be tested on three separate samples. Testing was performed on each sample three times during DC breakdown testing, for a total of 9 tests. Note that the same sample was tested three times and it is clearly possible that the first breakdown could have affected the second and third breakdown voltages. The hi-pot tester was setup to repeat the experiments automatically and the individual voltages were not recorded but were observed visually during testing. When the second and third breakdowns were less than the first, it was documented that there are outliers. The three breakdown measurements made on each sample were averaged, with the outlier breakdowns documented separately. In hindsight, the breakdown voltages should have all been documented but it was

assumed that because the threshold breakdown current from the hi-pot tester is so low, it would not cause significant arcing damage to the insulator such that it would impact future breakdown events. This might have been an ambitious assumption, but it was too late by the time it was realized.

4.2.1 Experimental Procedure – Hi-pot Testing

The test benches previously described earlier were installed into the cabinet of the hi-pot tester for sample testing and connected to the positive and negative copper rails via banana connectors to the positive and negative nodes of the hi-pot tester. The hi-pot tester cabinet shelf is a layer of 1/4" thick polycarbonate on top of which a 40-mil sheet of PVC shower liner was placed to protect the cabinet shelf from the testbench as well as to reduce the sliding movement capabilities of the test bench.

The dry polluted samples were loaded into the testbench by separating the fiberglass brackets along the slotted base and placing the sample on the edge of the ceramic blocks in between the copper rails. The brackets were then pressed together at either edge of the sample, evenly along each edge to ensure a solid connection between the sample and the copper rail, and the brackets bolts were then tightened down to keep the brackets securely in place.

After the testing for each dry polluted sample was complete, a wet test was performed. The dry sample was left in place and a small amount of tap water was applied to the surface via a syringe with the droplets being applied evenly across the surface. For the 18.5 mm width samples 0.4mL was applied, producing an average of 0.03 mL/cm^2. To maintain a similar liquid density, the 43.5 mm width samples had 1.0 mL applied, producing a similar average of 0.03 mL/cm^2. The tests were repeated for the wet samples with the same test controls.

The test controls on the hi-pot tester allow for configuring of a maximum test voltage, the ramp rate (kV/s) to reach the maximum test voltage, and the dwell time for which to hold at the maximum test voltage. The maximum test voltage for each set of samples and pollution levels was determined empirically and set high enough that the sample experiences breakdown prior to reaching the maximum voltage; a breakdown due to voltage dwell time was deemed undesirable for the test results. The ramp rate was typically set to 1 kV/s for all samples and pollution levels. The hi-pot tester registers a breakdown event as having occurred once 5 mA of leakage current passes between the copper rails which is typically accompanied by a noticeable *crack* sound and a visible discharge. Some examples of breakdowns captured optically using an in-situ webcam are shown below in Figures 35 and 36. Note that not all breakdowns occurred across the sample, as seen in Figure 36.

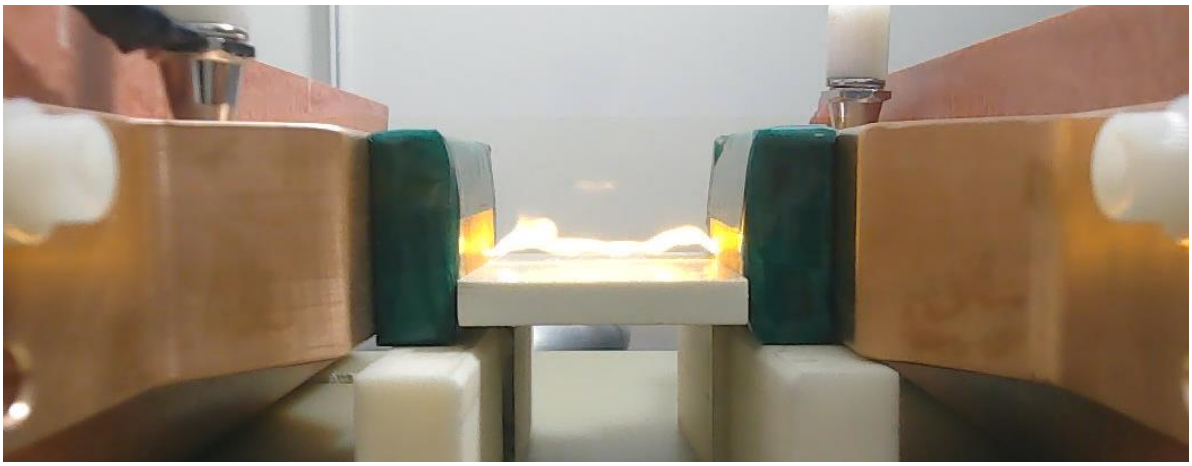

Figure 35 – Surface flashover of a polluted G9 sample

Figure 36 – Breakdown across the top of the electrodes

4.2.2 Experimental Procedure – Pulsed Power Testing

Samples that experienced breakdown during DC testing within 12 kV were selected for testing in the pulsed power environment. This range was selected as the testing is performed up to 9 kV in the pulsed power test bench due to the limitations of the capacitors used. By selecting components that experienced DC surface flashover up to 12 kV, an increase of 33.3% over the pulsed power maximum, the difference in breakdown characteristics between the ramped DC and the pulsed power test benches can be investigated.

The samples selected for testing were polluted using the same methods previously described and tested under the DC test conditions for both wet and dry pollutants. The capacitors were charged and triggered in 500 V increments until a breakdown is induced or 9 kV is reached. The energy stored in the two capacitors is high, 67 kJ at 9 kV charge, causing significant damage to the insulators and the copper electrodes during an experiment, shown earlier and again in Figure 37. This made testing this way very expensive and slow.

Figure 37 – Polluted Delrin® sample loaded into pulsed power testbench (left), after breakdown (right)

CHAPTER V

EXPERIMENTAL RESULTS

During the DC testing in the hi-pot tester, the samples experienced three outcomes: surface flashover, edge tracking, and through tracking. Surface flashover was the most common and desired outcome, whereas the edge and through tracking demonstrated the inconsistency in the breakdown phenomena. Edge tracking occurred on G10 and G11 samples where an edge burr was left after the sample was cut to size using a table saw or bandsaw. The edge of the sample is unable to hold off the voltage and fails quickly, typically between 1 - 2 kV for the smaller width samples. Once the edge gives, a path is created for the current to pass through and the sample is no longer usable, seen in Figure 38. This failure was initially mitigated by ensuring that the edge burrs were removed by sanding; after the samples were cut to size using a waterjet the burrs were no longer left behind and edge tracking ceased.

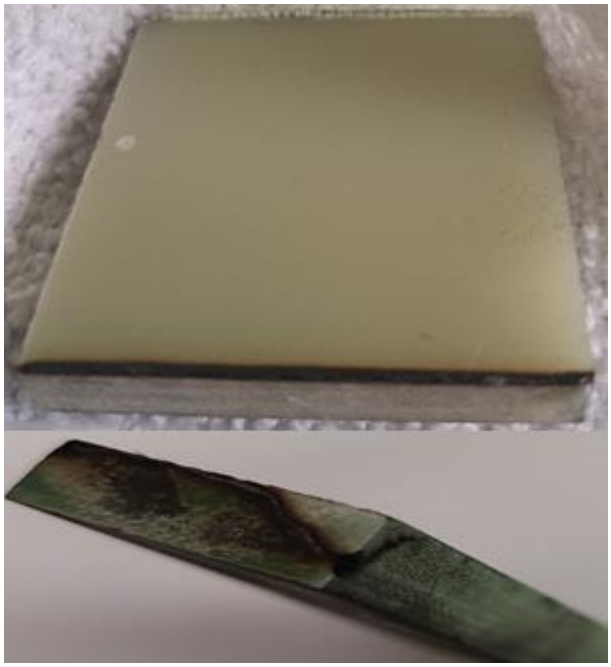

Figure 38 – G10 (top) and G11 (bottom) samples that experienced edge tracking

Through tracking was an undesired outcome experienced during the first round of salt fog testing, and it occurred exclusively on salt-fog polluted G9 samples of all sizes. Due to the layered nature of the G9 samples, the layers saturate with moisture from the salt fog chamber and never fully dry. When the sample undergoes testing, the polluted inner layers of the sample allow for the current to pass through the middle at low voltages, between 1 - 3 kV, seen in Figure 39. To mitigate this issue, the samples were removed from the salt-fog chamber to dry after the salt-fog application. This allowed for the salt-fog to pollute the surface of the samples but not penetrate and saturate the middle layers. No through tracking was experienced after this change in pollution application.

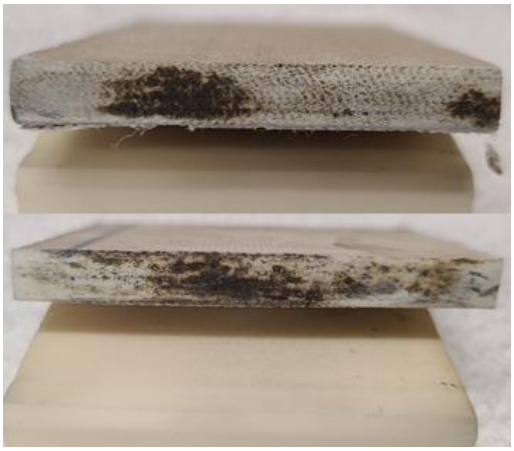

Figure 39 – G9 samples that experienced through tracking

5.1 Round 1 DC Test Results

The first round of testing was performed on unpolluted samples, as well as salt-fog (NaCl), carbon dust, and kaolin clay polluted samples. The data collected during the first round of testing for each material type is shown in Figure 40 through Figure 44. A few images taken during experiments performed on unpolluted G11 are shown in Figure 45. The measured data is compared with the predicted measurement from UL 840 assuming pollution level 1, the highest suggested voltage for a given gap distance, and material type 1. The salt-fog polluted G9 samples of all sizes experienced through tracking causing early overcurrent breakdowns in the test chamber. No

surface flashover occurred on these samples. The breakdowns on these samples occurred near the interpolated UL 840 pollution degree 1 operating voltage rating of 4.625 kV for 18.5 mm and 10.75 kV for 43 mm, with each size experiencing sample breakdowns slightly above and below the ratings. A more conservative rating of pollution degree 3, where the salt-fog pollution would likely be considered, leads to a maximum operating voltage of 1.468 kV, a full 1 kV below the lowest through-tracked G9 bulk breakdown. This data suggests that in most cases, UL 840 is overly conservative in its voltage prediction since even most of the polluted samples broke down at a higher voltage than pollution level 1 suggests. Keep in mind that it is so difficult, if not impossible, to really correlate how UL 840 accounted for CTI, PLC, and pollution type in their experiments for a true correlation to be made. This clearly illustrates the issue with using standards such as UL 840 for just any application.

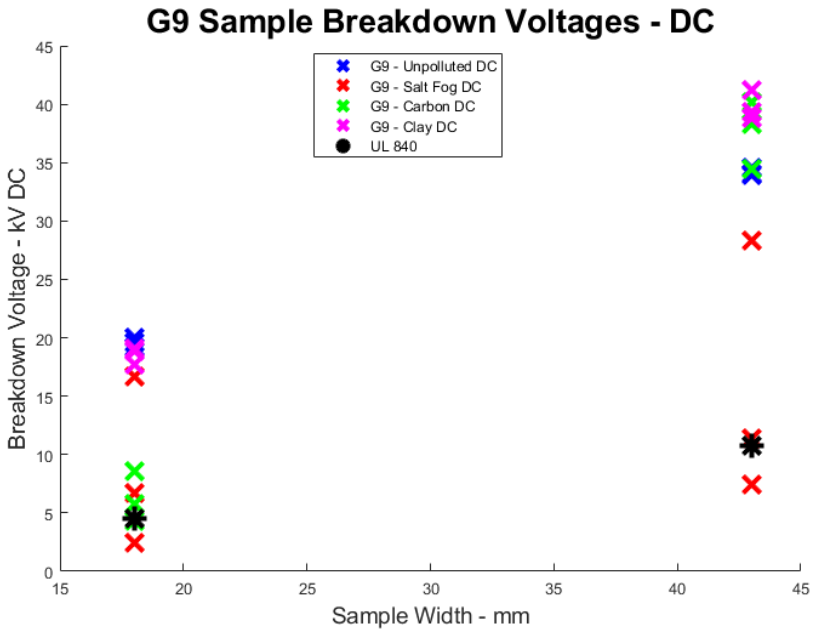

Figure 40 – G9 DC Breakdown – Round 1

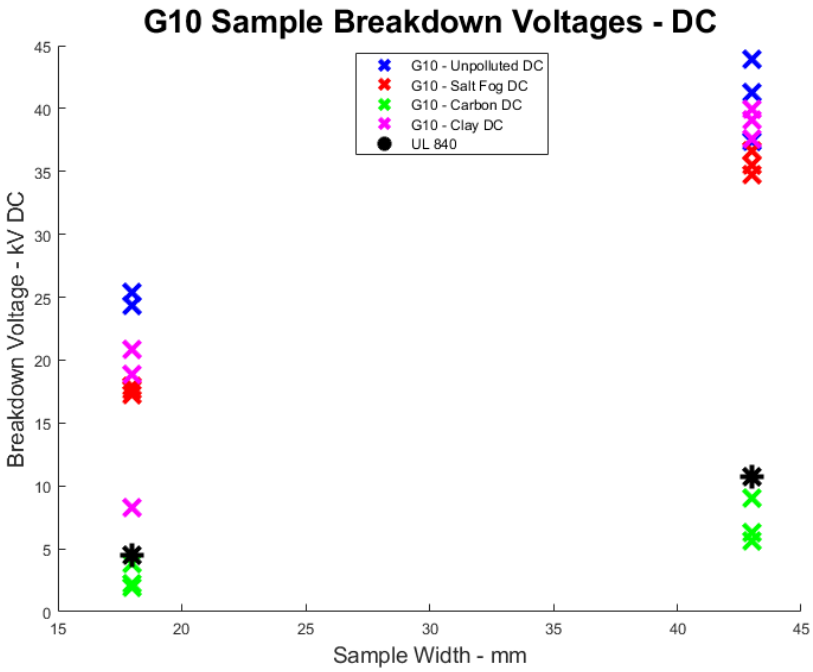

Figure 41 – G10 DC Breakdown – Round 1

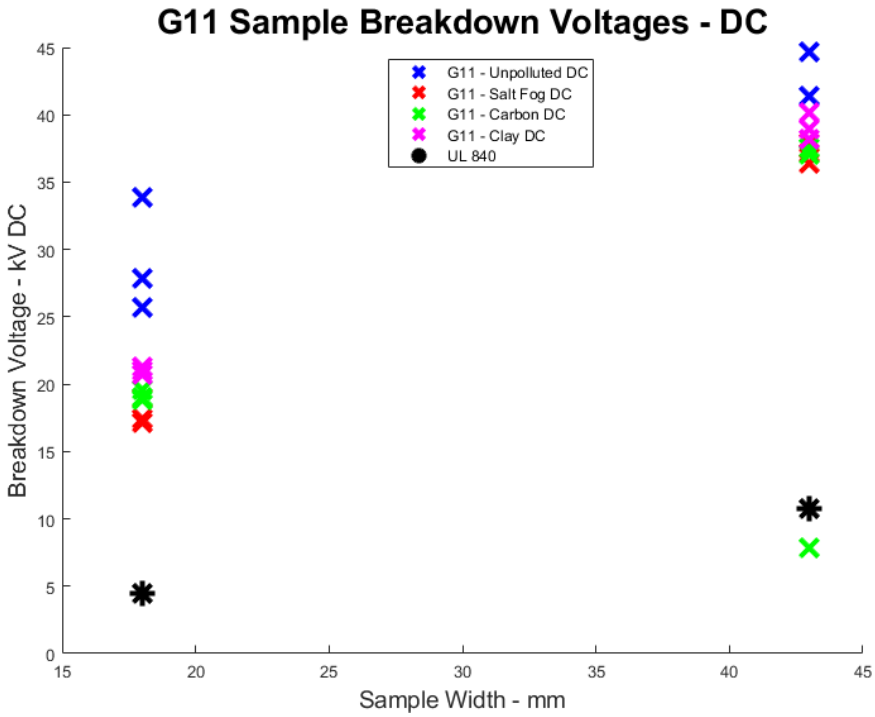

Figure 42 – G11 DC Breakdown – Round 1

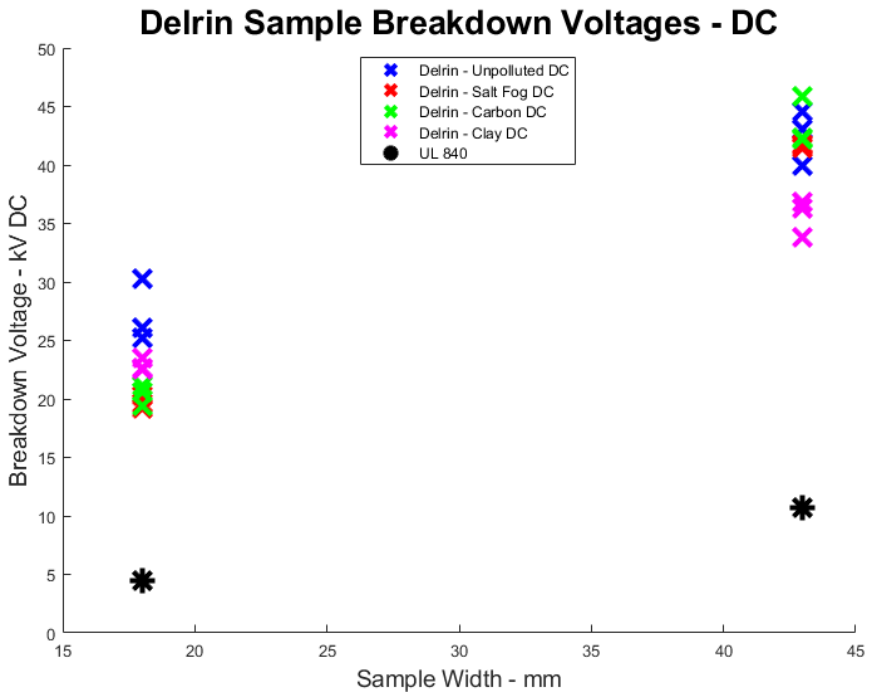

Figure 43 – Delrin® DC Breakdown – Round 1

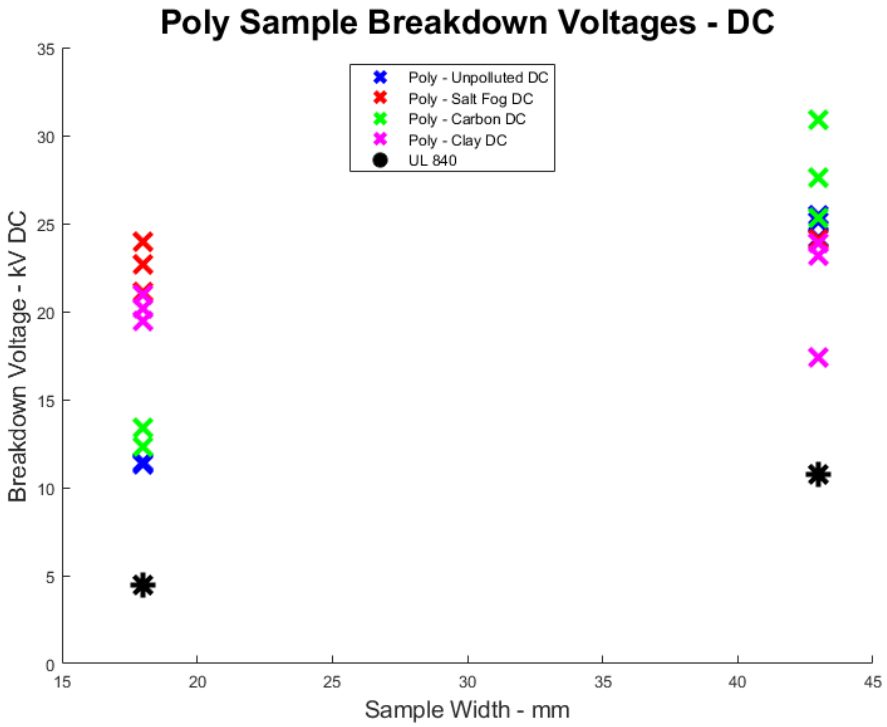

Figure 44 – Polycarbonate DC Breakdown – Round 1

The carbon dust pollution had varying effects on the samples depending on the insulator tested; G9, G10, and G11 carbon dust polluted samples exhibited breakdown voltages lower than

the unpolluted baseline samples, whereas the Delrin® and polycarbonate carbon dust polluted samples experienced higher-than-baseline breakdown voltages. The carbon dust pollution also contributed to the edge tracking samples, which occurred on two G11 samples, one G10 sample, and one polycarbonate sample. Replacement samples were made, with focus on removing and reducing edge burrs, and retested. The edge tracking potential of carbon dust polluted samples is worth noting, however.

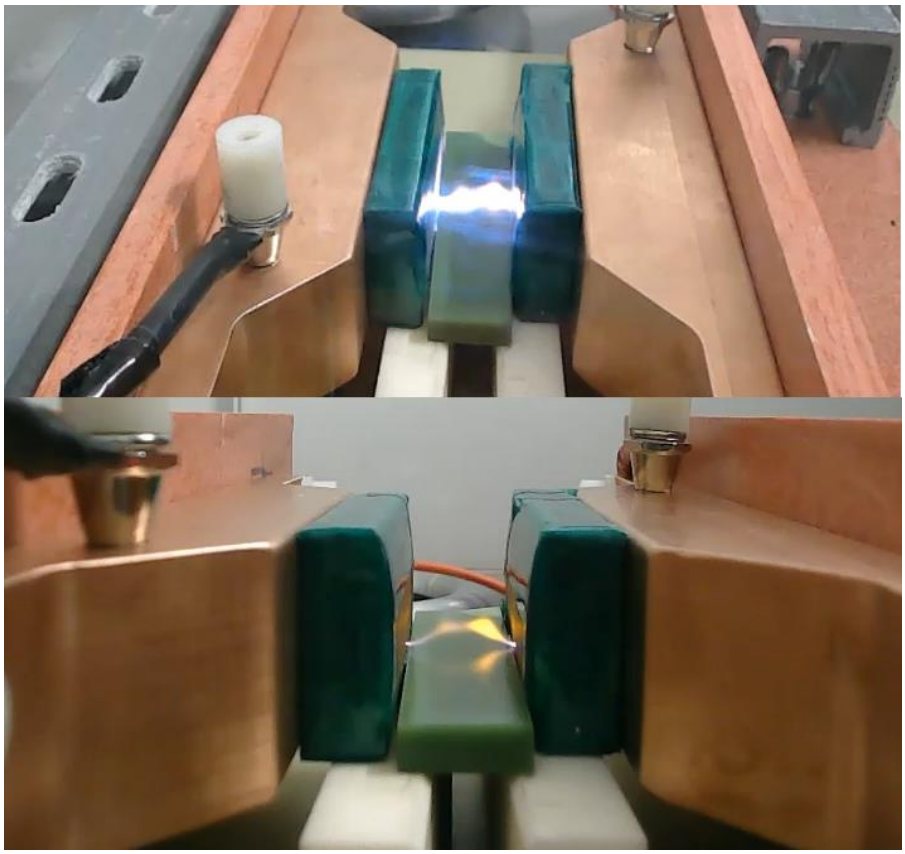

Figure 45 – Surface flashover of an unpolluted G11 sample from two angles

The polycarbonate samples produced the largest variance in breakdown voltages, with minimal overlap between the various levels of pollution. The pollution levels appear as separate groupings on the plot for both sizes tested. Contrarily the G9 samples exhibited significant overlap

of pollution level testing; apart from the salt-fog tested samples that experienced through tracking, each level of pollution could breakdown at seemingly any voltage.

Kaolin clay coated samples did not exhibit a consistent, significant change compared to the unpolluted samples; some samples experienced a lower breakdown voltage, others a higher one. This was to be expected, as the kaolin clay pollution testing was selected to verify the IEC 60507 recommendation for kaolin clay usage as an inert material intended to have minimal effect on breakdown voltage, to improve the adherence of other pollutants to the insulator surfaces.

5.2 Round 2 DC Test Results – Dry Pollution

The experimental data collected during the second round of DC flashover experiments performed using the hi-pot tester are shown in Figure 46 through Figure 50. As in the first round of data, the interpolated UL 840 pollution degree 1 operating voltage of 4.625 kV for 18.5 mm was selected for comparison to the polluted sample breakdown results and 10.75 kV was interpolated for use as the 43 mm pollution degree 1 breakdown. The use of pollution degree 1 for comparison again visibly demonstrates the conservativeness of the UL 840 standard for this round of testing, as the closest breakdown voltage of dry pollutants, that of the iron powder used to meet the pollution degree 4 requirements, occurred at more than double that of the pollution degree 1 requirements. When compared to the pollution degree 4 requirements for the distances tested the iron powder pollution breakdowns occurred at voltages 10 - 20 times higher than the voltages listed in the UL 840 pollution degree 4 creepage distance table. The iron powder pollution produced the lowest breakdown voltages overall, as expected. All iron powder samples experienced breakdown voltages lower than that of the unpolluted test samples, whereas some samples experienced occasional higher breakdown voltages when polluted with $CaSO_4$ and NaCl salts. Movement of the iron powder under the influence of electric and magnetic fields throughout

experiments was clearly captured using the webcam inside the chamber. A timelapse collection of still images during an experiment are shown in Figure 51. It is worth noting that cleanup after each of those iron powder experiments was time consuming due to the mass movement of the powder all over the chamber. Eventually a scheme was devised to contain the powder so that cleanup time could be minimized.

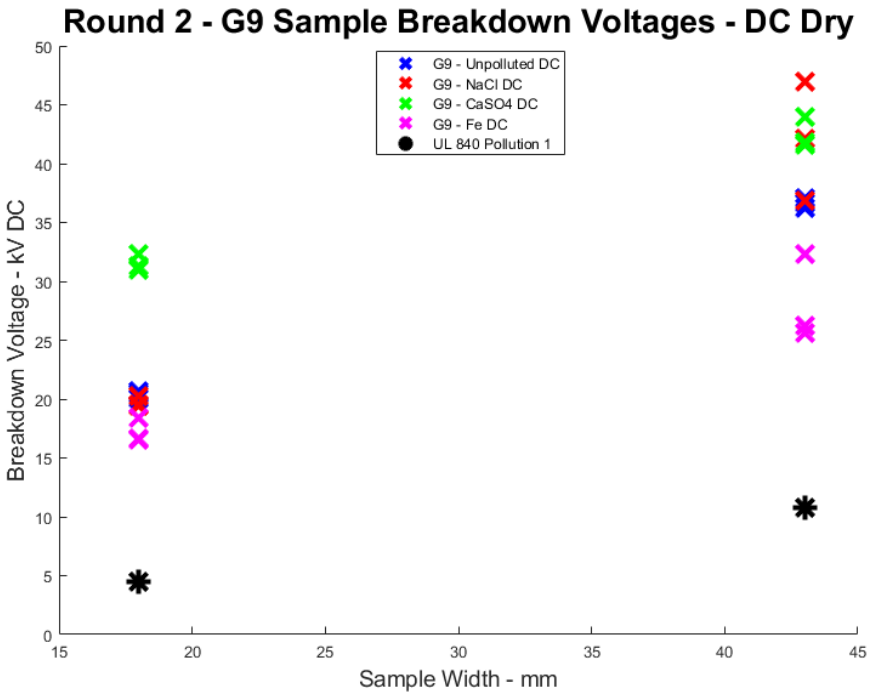

Figure 46 – G9 DC Breakdown – Round 2 Dry

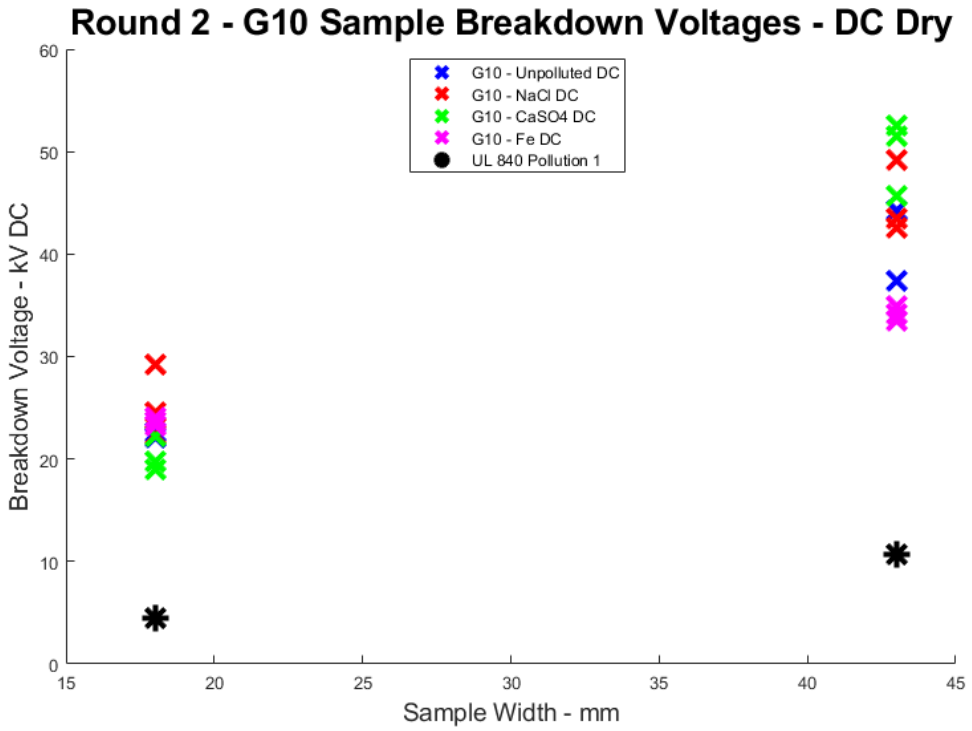

Figure 47 – G10 DC Breakdown – Round 2 Dry

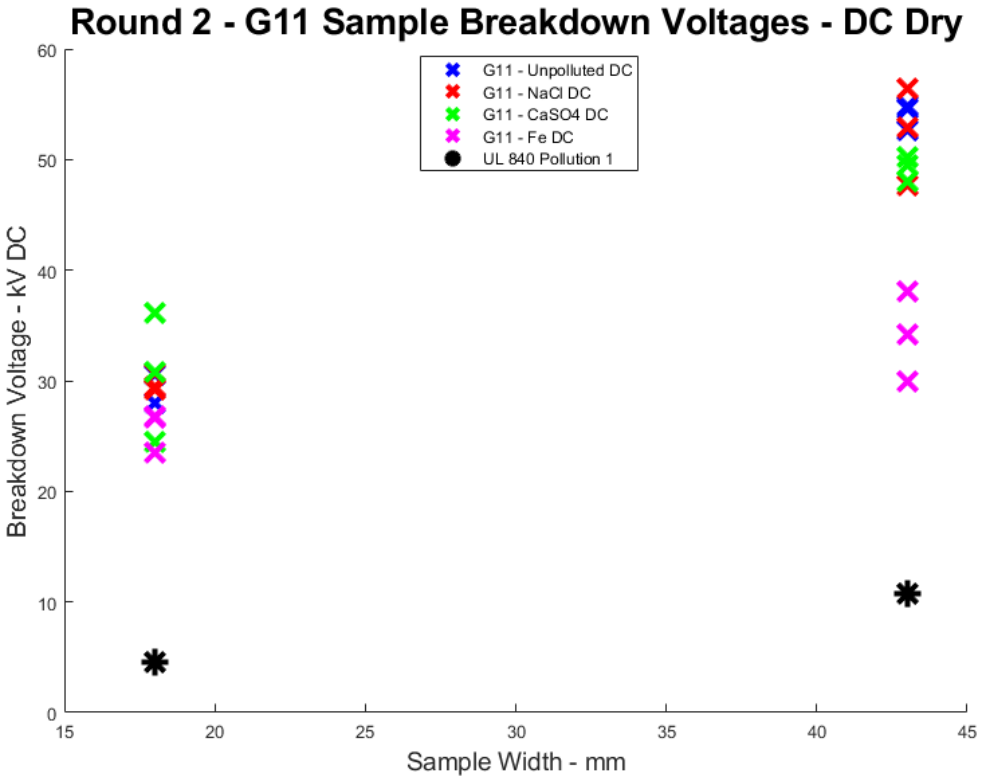

Figure 48 – G11 DC Breakdown – Round 2 Dry

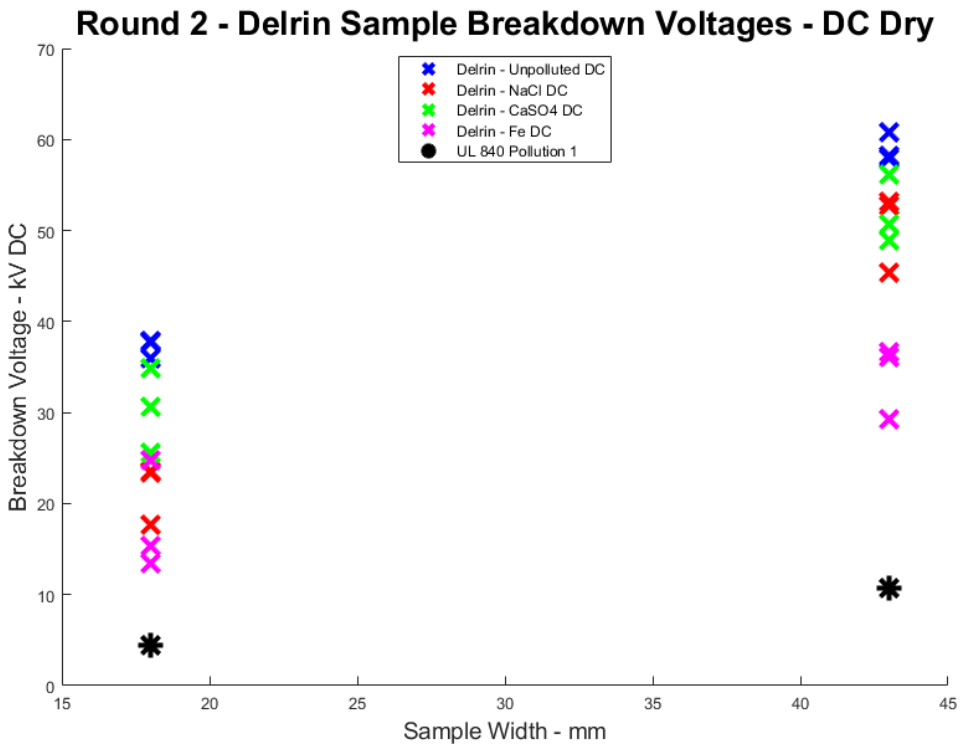

Figure 49 – Delrin® DC Breakdown – Round 2 Dry

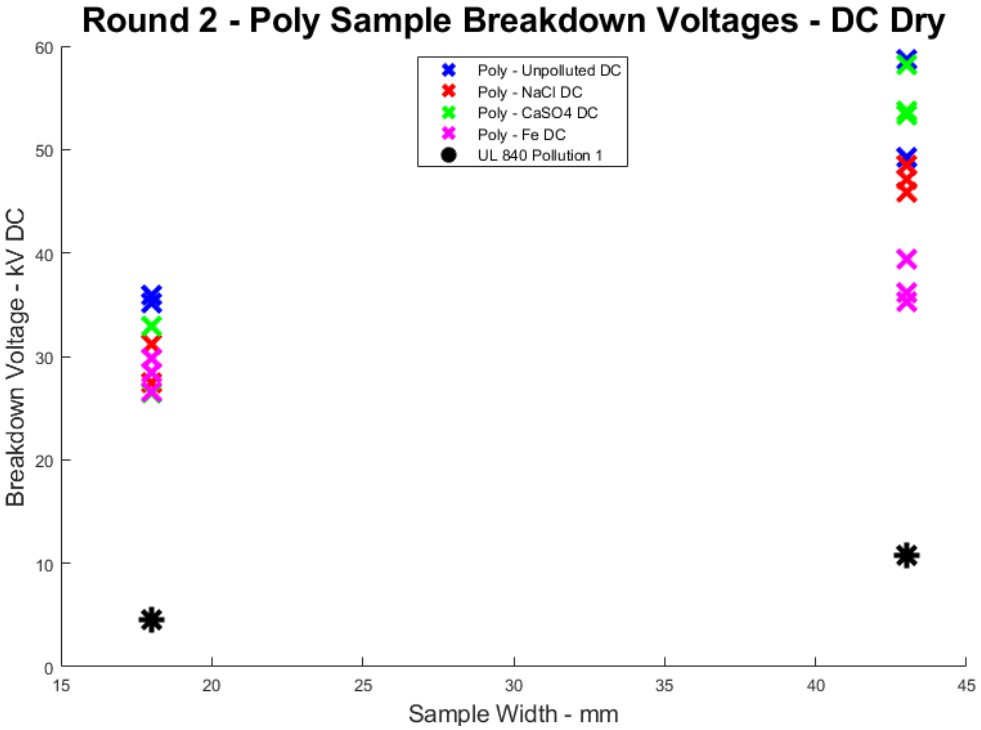

Figure 50 – Polycarbonate DC Breakdown – Round 2 Dry

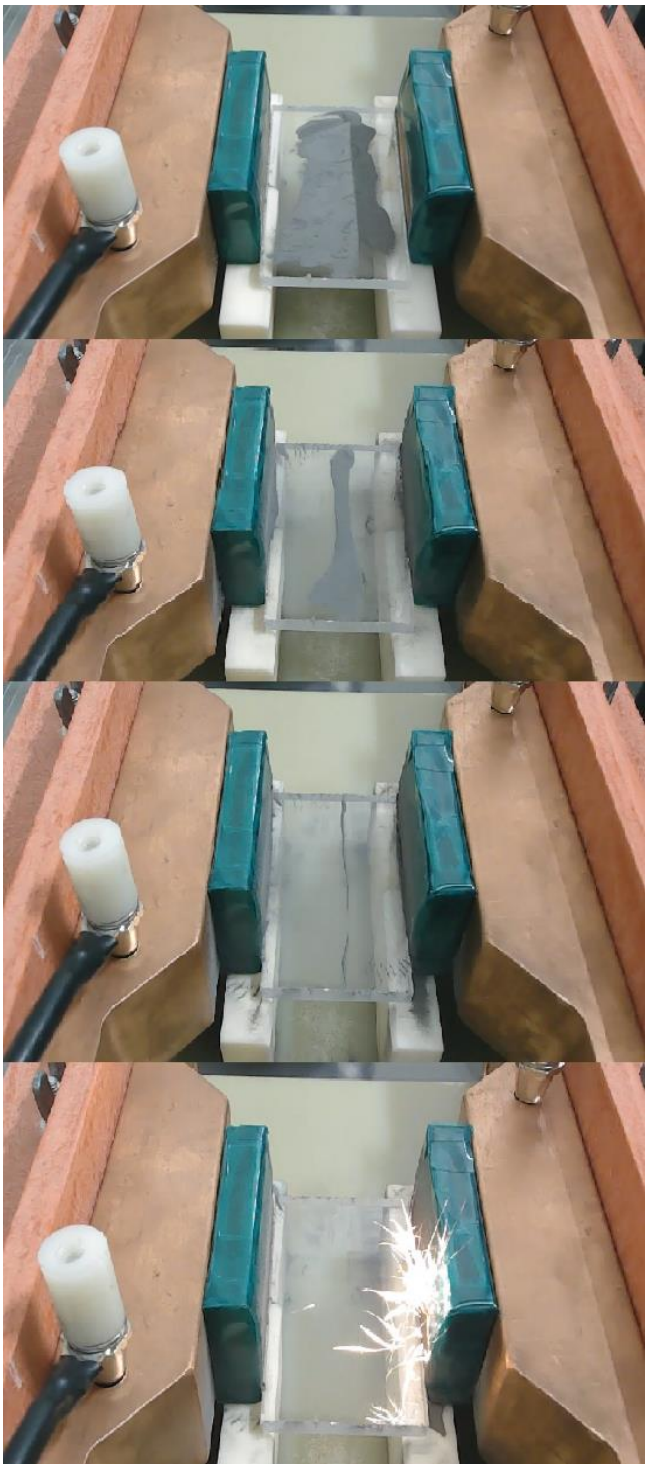

Figure 51 – Breakdown sequence of iron powder polluted polycarbonate sample. The iron powder moves across the sample and to the face of the electrodes as the magnetic field increases.

5.3 Round 2 DC Test Results – Wet Pollution

The interpolated breakdown voltages for pollution degree 4 were selected for comparison of the wet sample testing. Pollution degree 4 is based on pollution generating persistent conductivity through rain and snow, which the application of the water droplets to dry polluted samples is intended to mimic; Material group 1 subsection was selected as it provides the most leeway and emphasizes the overconservative recommendations of UL 840. All wet samples of all pollution degrees experienced voltage breakdown at levels at least double those listed as the minimum requirements. The results from the wet DC tests are shown in Figure 52 to Figure 56.

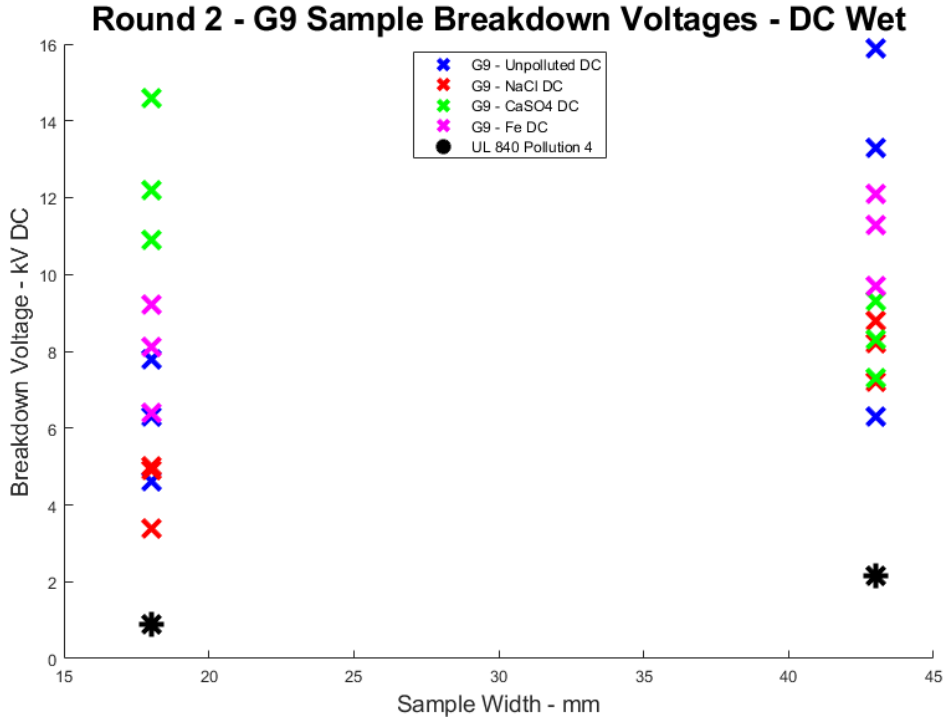

Figure 52 – G9 DC Breakdown – Round 2 Wet

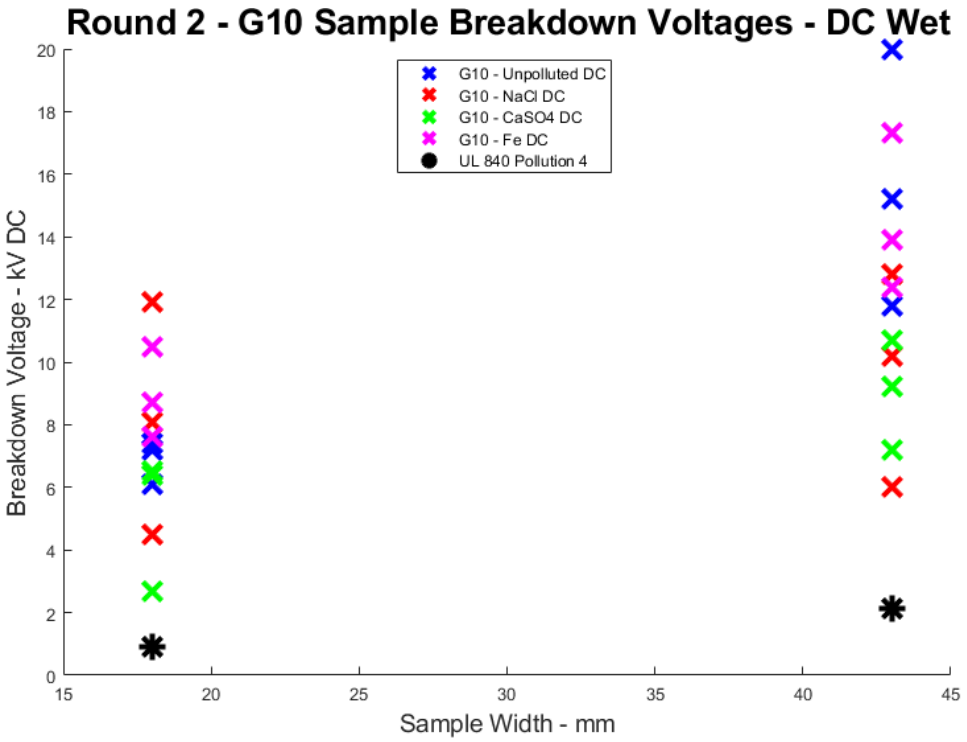

Figure 53 – G10 DC Breakdown – Round 2 Wet

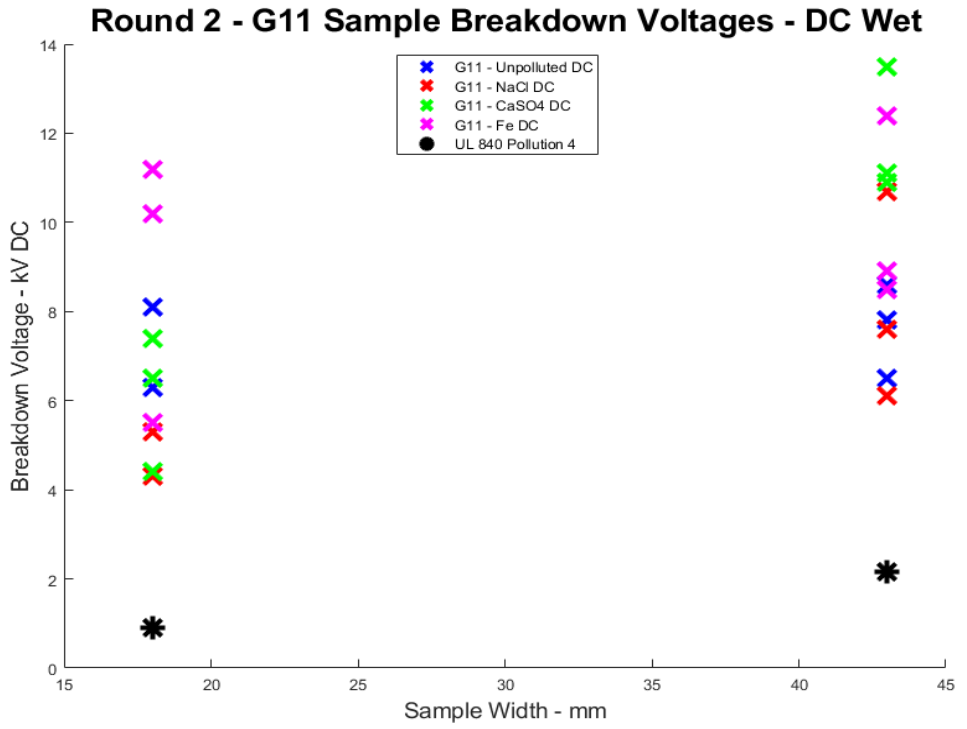

Figure 54 – G11 DC Breakdown – Round 2 Wet

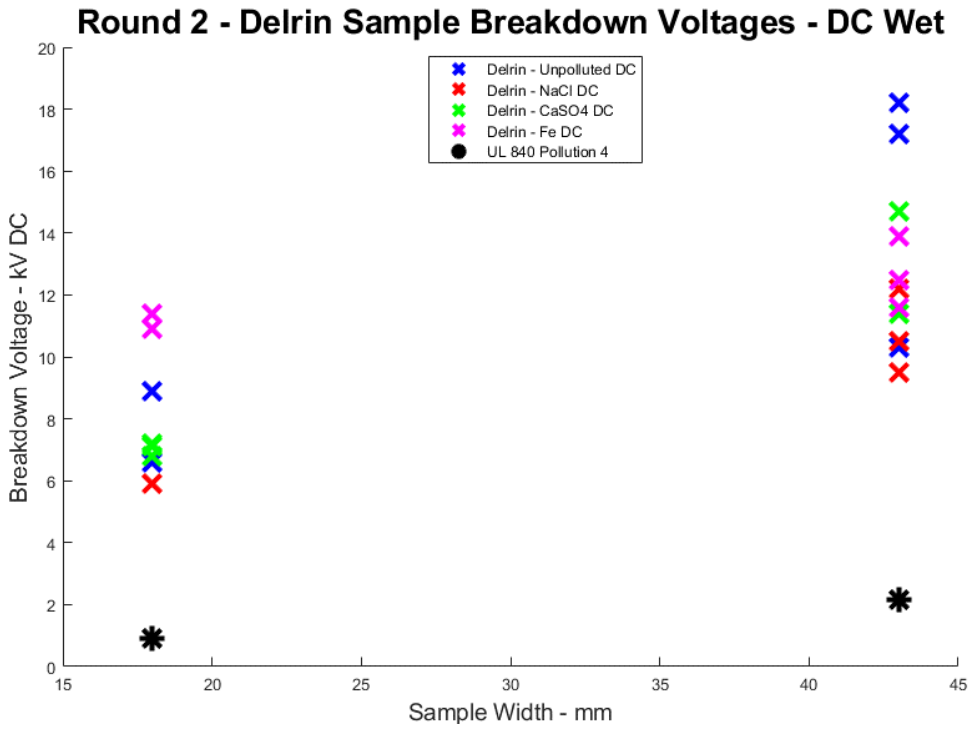

Figure 55 – Delrin® DC Breakdown – Round 2 Wet

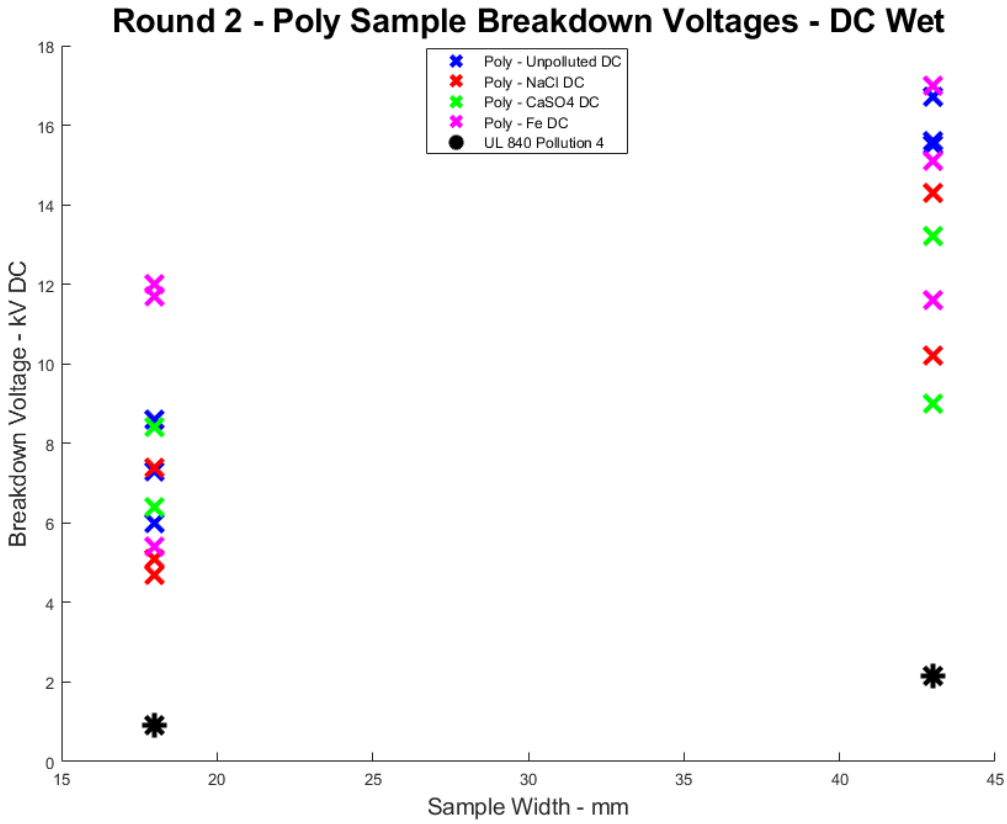

Figure 56 – Polycarbonate DC Breakdown – Round 2 Wet

The difference in breakdown voltage between dry and wet pollution testing was smallest for iron powder polluted samples. A photograph captured from the webcam during a wet iron powder experiment is shown in Figure 57. In the dry testing, the iron powder samples generally experienced the lowest breakdown voltages, whereas under wet testing the breakdown voltages were generally higher than unpolluted wet samples and this is likely due to reduced mobility of the iron powder.

The calcium sulfate polluted samples typically experienced the largest drop in breakdown voltages between dry and wet pollution. This fits expectations as insulators polluted with $CaSO_4$ are documented to have a greater dependency on steam input-rate, which leads to surface moisture, than NaCl polluted insulators [28]. A photograph taken during a wet NaCl pollution experiment is shown in Figure 58.

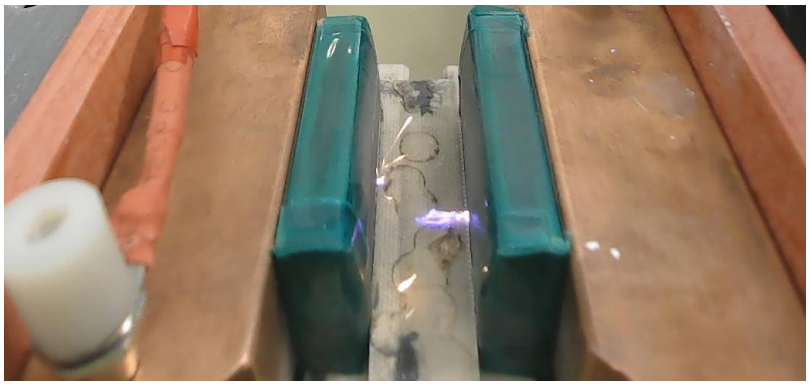

Figure 57 – Wet iron powder pollution breakdown on G9 sample

Figure 58 – Wet NaCl pollution breakdown on polycarbonate sample

5.4 Round 2 Pulsed Power Test Results

The samples selected for higher-energy transient voltage testing were those that experienced breakdowns in the DC testing environment under 12 kV, with the list of those and the test results seen below in Figures 59 and 60. From the first round of testing only the 18.5 mm carbon-coated polycarbonate sample fell within this range and those never did breakdown in the pulsed-power test environment.

As the second round of DC testing encompassed all documented degrees of pollution, a larger portion of polluted samples produced flashover results within the test range for the pulsed-power environment. Four of the five dry iron powder, pollution degree 4, samples tested experienced breakdown without the added presence of water at 18.5 mm, with all 5 samples at the same size undergoing surface flashover with the addition of water to the dry pollution. These breakdowns all occurred at or below 5 kV, a significantly reduced voltage compared to the DC breakdown testing. In general, all pollution levels tested under the pulsed-power conditions experienced breakdowns at reduced voltages compared to their DC-tested counterparts. Similarly, four of the five samples tested at the 43 mm size with the moisture added iron powder experienced flashover, again at voltages below the equivalent DC breakdowns. This is believed to be due to the significantly increased rate of voltage vs time the fields are applied at. A photograph of a G10 sample polluted with iron powder and water before and after a pulsed breakdown test is shown in Figure 61.

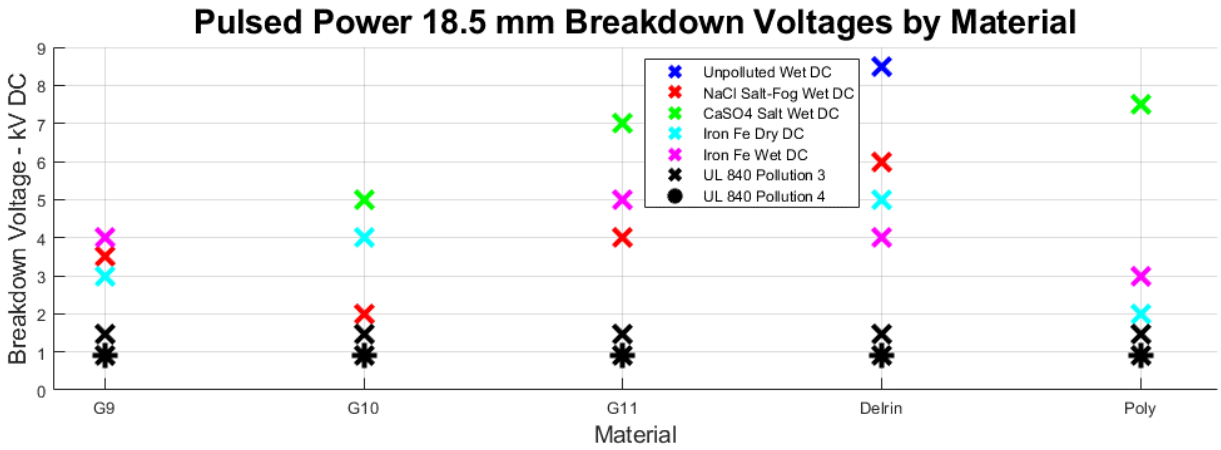

Figure 59 – Pulsed power breakdown voltages by material – 18.5 mm samples

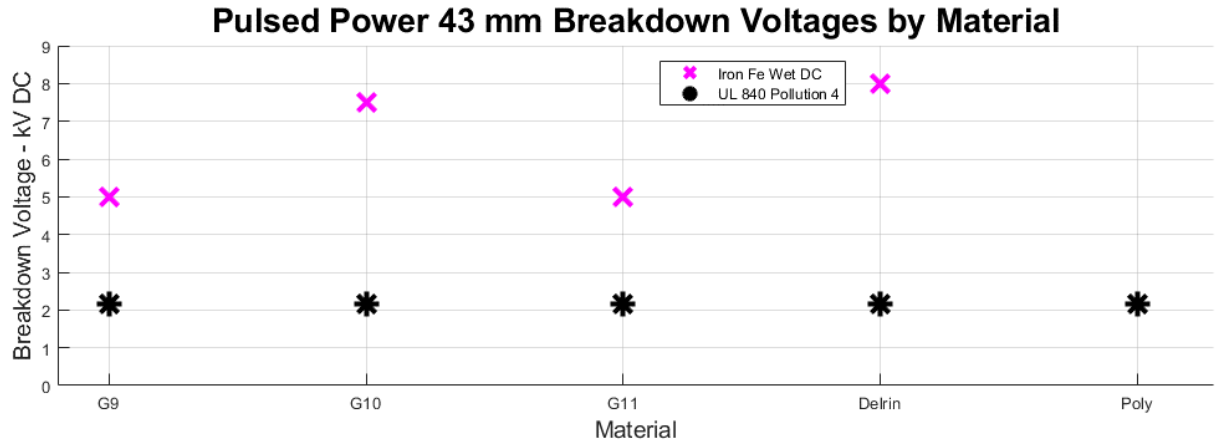

Figure 60 – Pulsed power breakdown voltages by material – 43 mm samples

The only unpolluted wet sample to breakdown under the pulsed power conditions was the 18.5 mm Delrin® sample. This breakdown was unexpected and uncharacteristic compared to both the results of the other sample testing as well as the DC breakdown results. Delrin® samples typically experienced breakdown at higher voltages than the other insulators tested, which was also the case for the unpolluted wet DC test.

Figure 61 – G10 sample polluted with iron powder and water. Before breakdown (left) and after breakdown (right). The lower part of the sample, where the breakdown occurred, is completely dry – a dry band formed during breakdown. The top of the sample, away from the breakdown, is still wet.

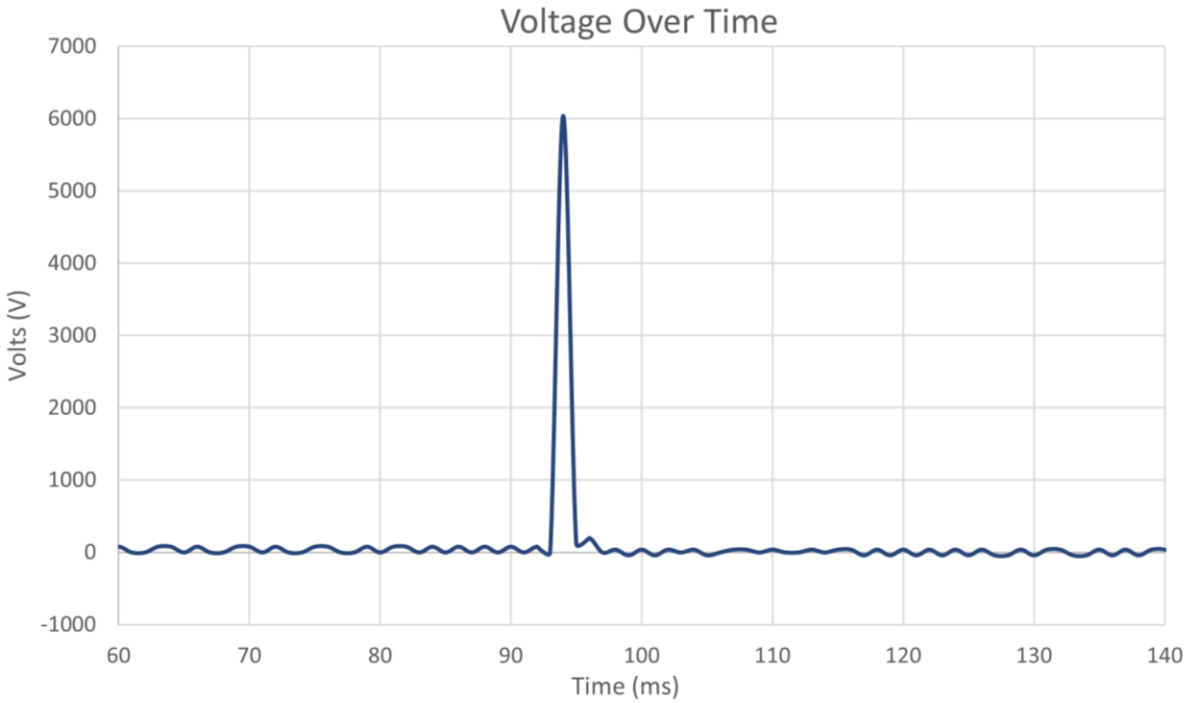

Figure 62 – Voltage readout from G10 sample breakdown from Figure 59. Breakdown occurred at 6 kV trigger. Readout taken from RIGOL DS1054 oscilloscope. 1 ms sample time.

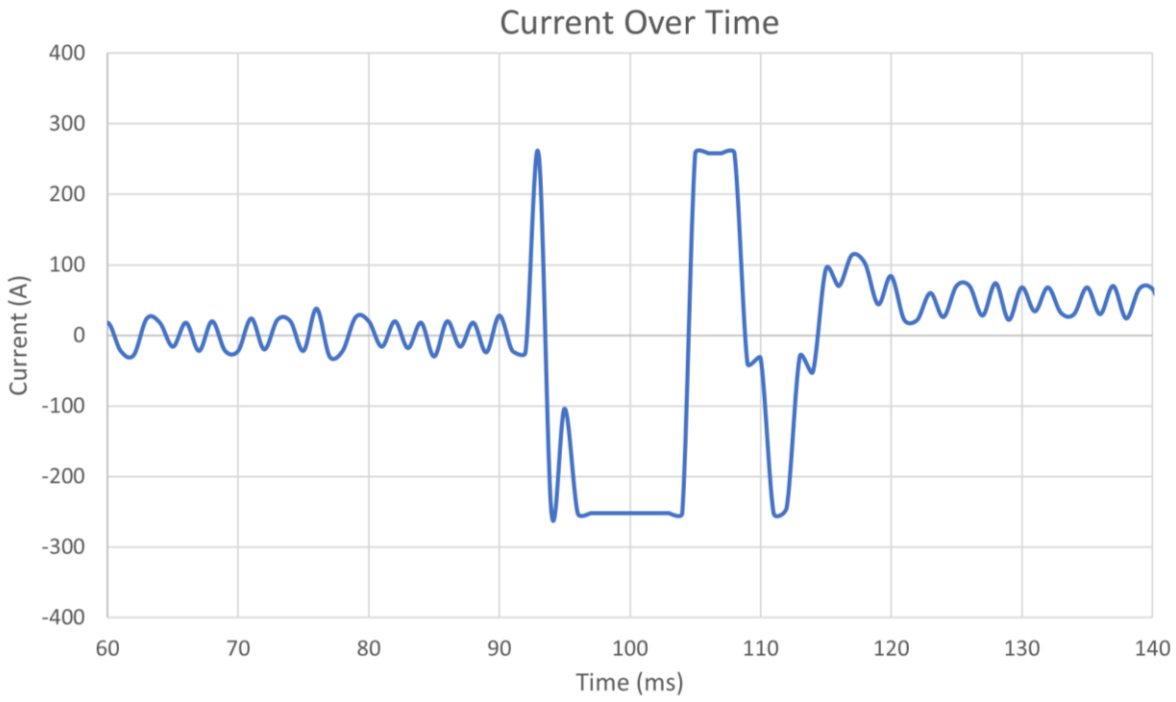

Figure 63 – Current readout from G10 sample breakdown from Figure 59. Breakdown current spiked to 258 A. Readout taken from RIGOL DS1054 oscilloscope. 1 ms sample time.

Figure 64 – G10 iron powder with water sample test. Oscilloscope readout from 3.5 kV trigger, 500 V below sample breakdown. Yellow curve displays voltage at 0.5X rate (2000X voltage probe with 1000X oscilloscope voltage probe setting), blue curve displays current at a reading of 0.1 V/mA. Probe reading displays voltage ringing without breakdown.

CHAPTER VI

SUMMARY AND CONCLUSIONS

The work presented here has shown that the creepage distances listed in UL840 are overly conservative and in some cases not applicable to a pulsed-power environment. Under DC testing it is seen that, for all pollution degrees and material groups, the UL 840 creepage and clearance distances have significant buffer built in, to the point of detriment of systems where space is a premium. For these systems the design team would benefit from performing testing under the expected conditions to appropriately minimize and reduce size and weight, while also mitigating the risk of surface flashover. Alternatively, for situations where size and weight are less of a constraint than time available, UL 840 can be generally applied to most AC or DC systems, provided that a thorough understanding of the insulators being used as well as an accurate expectation of both pollutants and corresponding pollution levels can be achieved.

In the pulsed-power testing it was shown that breakdowns occurred at levels at or below the standard DC system counterparts, as well as UL 840 standards. For pulsed power systems UL 840 can not and should not be directly applied without prior testing. These shortfalls compound the difficulty of application of the standard, such as the vague pollution degree definitions and sliding scale material groupings. Therefore, materials used in such environments need to be further tested under the expected conditions to determine longer term applied voltages as well as an appropriate cleaning or replacement schedule for the materials subjected to naval conditions.

REFERENCES

[1] *Standard test method for high-voltage, low-current, dry arc resistance of solid electrical insulations*, ASTM D495-99, 1999.

[2] *Dry, solid insulating materials – resistance test to high-voltage, low-current arc discharges*, IEC 61621:1997, 1997.

[3] *Polymeric materials – short term property evaluations*, UL 746A, 2001.

[4] *Insulation coordination including clearances and creepage distances for electrical equipment*, UL 840, 2007.

[5] *Electrical insulating materials used under severe ambient conditions – test methods for evaluating resistance to tracking and erosion*, IEC 60587, 2007.

[6] *Standard test method for comparative tracking index of electrical insulating materials*, ASTM D3638-21, 2021

[7] *Method for the determination of the proof and the comparative tracking indices of solid insulating materials*, IEC 60112:2003, 2003.

[8] *Standard test method for dust-and-fog tracking and erosion resistance of electrical insulating materials*, ASTM D2132-03, 2003.

[9] J. Kuffel and P. Kuffel, *High voltage engineering fundamentals.* Elsevier, 2000.

[10] T. Damle, C. Park, J. Ding, P. Cheetham, M. Bosworth, M. Steurer, R. Cuzner, and L. Graber, *"Experimental setup to evaluate creepage distance requirements for shipboard power systems",* in IEEE Electric Ship Technologies Symposium, Washing, DC, USA, 2019.

[11] D. Boesing, *"Creepage and clearance and connectors,"* The Samtec Blog, 13-May-2019. [Online]. Available: https://blog.samtec.com/post/creepage-clearance-connectors/.

[12] *"A game-changing flashover prediction technology for power utilities,"* Metrycom. [Online]. Available: http://www.metrycom.com/disruptive-flashover-prediction.

[13] *"Overview of failure modes of porcelain, toughened glass & composite insulators,"* INMR, 30-Jun-2017. [Online]. Available: https://www.inmr.com/overview-failure-modes-porcelain-toughened-glass-composite-insulators/.

[14] J. Krile*, "Physics of dielectric surface flashover at atmospheric pressures",* M.S. thesis, Dept. Elect. Eng., Texas Tech Univ., Lubbock, TX, USA, 2003.

[15] Miller, H., *"Surface flashover of insulators,"* IEEE Transactions on Electrical Insulation, Vol. 24, No 5, pp. 765-786, October 1989.

[16] Hegeler,F., Masten, G., and Krompholz, H., "Current, Luminosity, and X-Ray Emission in the Early Phase of Dielectric Surface Flashover in Vacuum," IEEE Transactions on Plasma Science, Vol 21, No 2, pp. 223-227, April, 1993.

[17] Hegeler, F., Krompholz, H., Hatfield, L., and Kristiansen, M., "Insulator Breakdown in a Simulated Low Earth Orbit Environment," 10th IEEE Pulsed Power Conference, Albuquerque, NM July 10-13, 1995.

[18] Anderson, R. A., and Brainard, J. P., "Mechanism of Pulsed Surface Flashover Involving Electron-Stimulated Desorption," J. Appl. Phys., Vol. 51, No. 3, March, 1980, pp.1414-1421.

[19] Neuber, A., Butcher, M., Hatfield, L., and Krompholz, H., "Electric Current in DC Surface Flashover in Vacuum," J. Appl. Phys., Vol. 85, No. 6, March, 1999, pp.3084-3091.

[20] J. Krile, L. McQuage, J. Walter, and A. Neuber, 'Short pulse High Power Microwave surface flashover,' 2009 IEEE Pulsed Power Conference, 2009.

[21] Maxstadt, F. W., "`Insulator Arcover in Air," Electrical Engineering, vol. 53, July 1934, pp. 1062-1068

[22] Akyuz, Mose, "Positive streamer discharges in air and along insulating surfaces: experiment and simulation," Ph.D dissertation, Eng. Physics., Uppsala University, Uppsala, Sweden, 2002.

[23] Hippauf, E., "Influence of Water on the Flashover Strength of Insulators," Z. Phys. 82, 803, 1933.

[24] Neuber, A., Krompholz, H., and Hatfield, L., "Dielectric Surface Flashover at Cryogenic Temperatures," Conference on Electrical Insulation and Dielectric Phenomena, Minneapolis, MN, October 19-20, 1997, pp. 575-578.

[25] H. Rodrigo, W. Baumgartinger, G.H. Heller, D.G. Crook, and S.L. Ranner, 'Surface Flashover of Cylindrical G10 Under ac and dc Voltages at Room and Cryogenic Temperatures,' IEEE Transactions on Applied Superconductivity, Vol. 21, No. 3, June 2011.

[26] S. Li, H. Sun, Y. Chen, F. Wang, Z. Jin, Y. Yin, L. Yao, and Z. Hong, 'Study of Surface Flashover and Breakdown Characteristics in Liquid Nitrogen for SFCL Application,' IEEE Transactions on Applied Superconductivity, Vol. 24, No. 3, June 2014.

[27] M.P. Wilson_, R.A. Fouracre, M.J. Given, S.J. MacGregor, I.V. Timoshkin, K.J. Thomas, M.A. Sinclair, and J.M. Lehr, 'Surface flashover of dielectric materials used in pulsed power research,' IEEE Pulsed Power Conference, 2007, Albuquerque, NM.

[28] *Polluted insulators: a review of current knowledge*, CIGRE 158, 2000.

[29] Obenaus F, Fremdschichtueberschlag und Kriechweglaenge, Deutche Elektrotechnik, vol. 4, 1958, pp. 135-136.

[30] F. A. Chagas, "Flashover mechanism and laboratory evaluation of polluted insulators under DC voltage", Ph.D. thesis, Dept. Elect. Eng., The University of Manitoba, Winnipeg, Manitoba, Canada, 1996.

[31] *Selection and dimensioning of high-voltage insulators intended for use in polluted conditions – Part 1: Definitions, information and general principles*, IEC/TS 60815-1:2008, 2008.

[32] SECOM. (www.secom.com.ar), "EEE01 tracking index test apparatus + IEC 60112 + CTI," SECOM. [Online]. Available: http://www.secom.com.ar/english/EEE01-tracking-index-test-apparatus-IEC-60112.php.

[33] "G9 Glass-Melamine Laminate," [Online]. Available: https://www.professionalplastics.com/G9GLASSMELAMINE.

[34] "G10/FR4 Sheets," [Online]. Available: https://www.professionalplastics.com/G10FR4SHEET.

[35] "G11/FR5 - NEMA Grade FR5." [Online]. Available: https://www.professionalplastics.com/FR5_NEMAG11FR5.

[36] "Polycarbonate Sheet - Standard Grade." [Online]. Available: https://www.professionalplastics.com/POLYCARBONATESHEET.

[37] "Delrin® Sheet & Rod (Acetal Homopolymer)." [Online]. Available: https://www.professionalplastics.com/DELRINSHEET-ROD.

[38] "G9 Fiberglass Melamine Laminate Sheet," MatWeb. [Online]. Available: https://www.matweb.com/search/DataSheet.aspx?MatGUID=33c53b8b82124d2ab575f9e6bf14b3e5&ckck=1.

[39] Norplex Micarta, "NP 509 Technical Data Bulletin", G5/G9 datasheet, Mar. 2021

[40] "G10 fiberglass epoxy laminate sheet." *MatWeb*. [Online]. Available: https://www.matweb.com/search/DataSheet.aspx?MatGUID=8337b2d050d44da1b8a9a5e61b0d5f85.

[41] Synthane Taylor, "Material Specification: Grade G10/FR4", G10/FR4 datasheet.

[42] "CTI Comparative Tracking Index and PTI Proof Tracking Index of base material". [Online]. Available: https://db-electronic.com/en/pcb-manufacturing_s56.htm.

[43] “G11 fiberglass epoxy laminate sheet.” MatWeb. [Online]. Available: https://www.matweb.com/search/DataSheet.aspx?MatGUID=3854ca1b7ba94714a2686e8bd57abc2e.

[44] K&E Plastics, “Specification – NEMA: G11”, G11 datasheet

[45] “Overview of materials for polycarbonate, molded.” MatWeb. [Online]. Available: https://www.matweb.com/search/DataSheet.aspx?MatGUID=

[46] “Overview of materials for polycarbonate, extruded.” MatWeb, [Online]. Available: https://www.matweb.com/search/DataSheet.aspx?MatGUID=501acbb63cbc4f748faa7490884cdbca.

[47] “Polycarbonate (PC).” [Online]. Available: https://www.ulprospector.com/plastics/en/generics/25.

[48] “Dupont performance polymers Delrin® 100 BK602 POM.” [Online]. Available: https://www.matweb.com/search/DataSheet.aspx?MatGUID=e6f654c5f65f45339e672f1f6ce7008c.

[49] DuPont, “Delrin® acetal resin”, Delrin® design guide module III

[50] *Artificial pollution tests on high voltage ceramic and glass insulators to be used on a.c. systems*, IEC 60507:2013, 2013.

[51] *Artificial pollution test for polymer insulators – results of round robin test*, CIGRE 555, 2013.

[52] D. Carroll, "Rainwater as a chemical agent of geologic processes; a review," in "Water Supply Paper," Report 1535G, 1962.

[53] W. Lampe, T. Höglund, C. Nellis, P. Renner, and R. Stearns, “Long-term tests of HVDC insulators under natural pollution conditions at the Big Eddy test center”, IEEE Transactions on Power Delivery, Vol. 4, No. 1, Jan 1989.

[54] Z. Zhang, H. Huang, X. Jiang, M. Chen, and J. Hu, “Analysis of the Pollution Accumulation and Flashover Characteristics of Field aged 110 kV Composite Insulators”, in Electrical Insulation Conference, Annapolis, MD, USA, 2011.